HHS Public Access

Author manuscript

Life Sci. Author manuscript; available in PMC 2022 April 28.

Published in final edited form as:

Life Sci. 2022 January 01; 288: 120153. doi:10.1016/j.lfs.2021.120153.

Induction of distinct neuroinflammatory markers and gut dysbiosis by differential pyridostigmine bromide dosing in a chronic mouse model of GWI showing persistent exercise fatigue and cognitive impairment

Elena V. Kozlova[a,b], **Bruno Carabelli**[a,1], **Anthony E. Bishay**[a,1], **Rui Liu**[c,d], **Maximillian E. Denys**[a], **John C. Macbeth**[c,e], **Varadh Piamthai**[c], **Meli'sa S. Crawford**[e], **Declan F. McCole**[e], **Nicole I. zur Nieden**[a], **Ansel Hsiao**[c], **Margarita C. Curras-Collazo**[a,*]

[a]Department of Molecular, Cell and Systems Biology, University of California, Riverside, CA, USA

[b]Neuroscience Graduate Program, University of California, Riverside, CA, USA

[c]Department of Microbiology and Plant Pathology, University of California, Riverside, CA, USA

[d]Graduate Program in Genetics, Genomics, and Bioinformatics, University of California, Riverside, CA, USA

[e]Division of Biomedical Sciences, School of Medicine, University of California, Riverside, CA, USA

[*]Corresponding author at: Department of Molecular, Cell and Systems Biology, University of California, Riverside, Riverside, CA 92521, USA. mcur@ucr.edu (M.C. Curras-Collazo).

[1]Co-second authors.

Declaration of competing interest

No competing interests to declare.

CRediT authorship contribution statement

Elena V. Kozlova: Investigation, Conceptualization, Formal analysis, Writing - original draft, Writing - review & editing, Visualization, Supervision, Project administration. **Bruno Carabelli**: Investigation, Conceptualization, Formal analysis, Writing - original draft, Writing - review & editing. **Anthony E. Bishay**: Investigation, Formal analysis, Writing - original draft Writing - review & editing, Funding acquisition. **Rui Liu**: Investigation, Formal analysis. **Maximilian Denys**: Investigation, Formal analysis, Writing - review & editing. **John C. Macbeth**: Investigation, Supervision, Formal analysis. **Varadh Piamthai**: Investigation. **Meli'sa S. Crawford**: Investigation, Formal analysis. **Declan F. McCole**: Investigation, Supervision, Funding acquisition. **Nicole I. zur Nieden**: Conceptualization, Funding acquisition, Writing-review & editing. **Ansel Hsiao**: Conceptualization, Investigation, Supervision, Formal analysis, Writing - original draft, Writing - review & editing, Visualization, Funding acquisition. **Margarita C. Curras-Collazo**: Investigation, Conceptualization, Formal analysis, Writing - original draft, Writing - review & editing, Visualization, Supervision, Project administration, Funding acquisition.

Dedications

In memory of Dr. Boles Bishay: husband, father, and physician.

Ethics approval and consent to participate

Care and treatment of animals was performed in accordance with guidelines from and approved by the University of California, Riverside Institutional Animal Care and Use Committee (AUPs 20170026, 20200020, 20180067 and 20200015).

Consent for publication

Not applicable.

Data deposition

Raw sequencing data has been deposited at NCBI BioProject under accession PRJNA705372.

Appendix A. Supplementary data

Supplementary data to this article can be found online at https://doi.org/10.1016/j.lfs.2021.120153.

Abstract

Aims: To characterize neuroinflammatory and gut dysbiosis signatures that accompany exaggerated exercise fatigue and cognitive/mood deficits in a mouse model of Gulf War Illness (GWI).

Methods: Adult male C57Bl/6N mice were exposed for 28 d (5 d/wk) to pyridostigmine bromide (P.O.) at 6.5 mg/kg/d, b.i.d. (GW1) or 8.7 mg/kg/d, q.d. (GW2); topical permethrin (1.3 mg/kg), topical N,N-diethyl-meta-toluamide (33%) and restraint stress (5 min). Animals were phenotypically evaluated as described in an accompanying article [124] and sacrificed at 6.6 months post-treatment (PT) to allow measurement of brain neuroinflammation/neuropathic pain gene expression, hippocampal glial fibrillary acidic protein, brain Interleukin-6, gut dysbiosis and serum endotoxin.

Key findings: Compared to GW1, GW2 showed a more intense neuroinflammatory transcriptional signature relative to sham stress controls. Interleukin-6 was elevated in GW2 and astrogliosis in hippocampal CA1 was seen in both GW groups. Beta-diversity PCoA using weighted Unifrac revealed that gut microbial communities changed after exposure to GW2 at PT188. Both GW1 and GW2 displayed systemic endotoxemia, suggesting a gut-brain mechanism underlies the neuropathological signatures. Using germ-free mice, probiotic supplementation with *Lactobacillus reuteri* produced less gut permeability than microbiota transplantation using GW2 feces.

Significance: Our findings demonstrate that GW agents dose-dependently induce differential neuropathology and gut dysbiosis associated with cognitive, exercise fatigue and mood GWI phenotypes. Establishment of a comprehensive animal model that recapitulates multiple GWI symptom domains and neuroinflammation has significant implications for uncovering pathophysiology, improving diagnosis and treatment for GWI.

Keywords

Central nervous system; Endotoxemia; Gut-brain axis; Gut microbiome; Probiotic; Intestinal permeability; Interleukins; Toxic wounds

1. Introduction

Gulf War Illness (GWI) is a chronic multisymptom illness afflicting one-third of the nearly 700,000 U.S. troops who served in Operation Desert Storm/Desert Shield in the 1991 Persian Gulf War (GW) [1]. The symptoms reported by ill GW veterans (GWVs) include memory, mood and attention impairment, profound fatigue, chronic muscle and joint pain, severe headaches, gastrointestinal disturbances, respiratory difficulties and chronic skin conditions [2,3]. Although no definitive cause for GWI has yet been established, the constellation of symptoms involving several organ systems, in combination with results from clinical studies using brain imaging, implicate an underlying central nervous system (CNS) pathophysiology. This includes microstructural alterations in the cortex, striatum, hippocampus and cerebellum, altered neuronal activity and elevated serum biomarkers of CNS damage, as well as a central neuroinflammatory state still present after 25 years since the GW [4,5].

Evidence strongly and consistently indicates that Gulf War neurotoxic exposures are causally associated with GWI. Of primary concern are the prophylactic use of pyridostigmine bromide (PB) pills and neurotoxic pesticides during deployment [2]. PB, an acetylcholinesterase (AChE) inhibitor (AChEI) and anti-nerve gas agent, was used prophylactically by U.S. and allied troops in the GW to protect against chemical warfare attacks. Indeed, GW-deployed veterans who reported taking PB, performed worse relative to GW-deployed veterans without PB use on executive system tasks involving attention, visuospatial skills, and visual memory [6]. The multi-neurotoxicant chemical exposures theory is supported by studies of animal models in which GWI-related chemicals (PB, permethrin and DEET) and mild stress cause cognitive and mood impairments [7,8]. Moreover, exposure to higher doses of PB, the insect repellent, DEET, and the insecticide permethrin and/or chlorpyrifos led to significant CNS damage in animal models of GWI [9,10]. The neurotoxic effects of GW agents include blood brain barrier disruption, increased cell death, impaired neurogenesis, mitochondrial dysfunction, reduced acetylcholine (ACh)-ergic markers in cortex, thalamus and hypothalamus and serotonergic (5-HT) and dopaminergic (DA) dyshomeostasis in nucleus accumbens and hippocampus [7,10–13]. Evidence also supports a dominant role for neuroinflammatory processes including activation of microglia and astrocytes in the CNS, which have key roles in the brain's inflammatory response [4,7,11–14]. GW chemicals PB, PB/PER or PER/DEET/CORT/DFP induce expression of neuroinflammatory markers in ventral hippocampus of rodents [15]. Pyrethroid pesticides such as permethrin, which were also widely used during the GW, can activate microglia in a Na+ channel-dependent manner to release TNF-α and induce central neurogenic inflammation [16]. Increased activation of immune cells is also observed in the brain of ill GWVs [2,17], while systemic biomarkers, such as elevated serum levels of pro-inflammatory cytokines, IL-1β, INF-γ, or IL-6 have also been reported [14,18–20]. An increased pro-inflammatory state is implicated as the underlying cause of cognitive impairment [21] and mood alterations in GWI [22], suggesting that GWI symptoms may be due to dysfunction of the innate immune system [22,20].

GWVs studied also complain of moderate or multiple fatigue symptoms (47%) and feeling unwell after exercise exertion (17%) [23]. However, the pathophysiology underlying the chronic fatigue domain of GWI has been difficult to ascertain since it has been understudied in experimental animals. In an accompanying article in this issue, we characterize enhanced exercise intolerance (fatigue) and GWI phenotypes associated with other symptom domains including cognitive impairment and mood alterations in the same mice after chronic exposure to GW agents [124]. A comprehensive animal model such as this, displaying the unique multi-symptom presentation of GWI, is critical for unraveling the underlying causes and for testing potential therapeutics [23,24].

Therefore, in this study, we evaluated the persistent modifications in gene expression related to neuroinflammation and neuropathic pain in our GWI model using real-time quantitative polymerase chain reaction arrays (RT-qPCR). We also examined brain levels of IL-6 using enzyme-linked immunoassay (EIA) and hippocampal astrogliosis measured using glial fibrillary acidic protein (GFAP) immunohistochemistry. The analyses were performed 6.6 months after GW exposure in order to increase translational relevance to ill GWVs who continue to suffer from cognitive and chronic fatigue symptoms 30 years after

exposure. Here, we show that two exposure regimens, differing in PB dosing (GW1, GW2), induce different underlying neuroinflammatory transcriptional signatures that correspond with dissimilar behavioral profiles described in our adjoining report [124]. Because recent reports indicate that gut-brain interactions may be implicated in promoting symptoms of GWI [24–28], we also examined GW agent-induced changes in gut microbiome community structure. Our results characterize gut dysbiosis signatures in GW1 and GW2, in parallel with systemic endotoxemia indicating gut-brain pathways may potentially contribute to phenotypic alterations. The ability to study different GWI symptom domains in association with altered neuropathological and gut microbiome profiles in the same animal model provides a new opportunity to establish the pathophysiology of GWI and to develop diagnostic markers and effective treatments that may involve probiotic therapy.

2. Materials and methods

2.1. Animal care and maintenance

C57Bl/6N mice were generated using breeders originally obtained from Charles River Labs (West Sacramento, CA) or Taconic (Germantown, NY). Mice were housed under standardized conditions (12:12-h light:dark cycle; lights on 07.00 h) in a specific pathogen-free vivarium with food and water available ad libitum. All experimental procedures were in strict compliance with NIH guidelines, and were approved by the University of California Riverside Institutional Animal Care and Use Committee (AUP#, 20210024, 20200020, 20180067)

2.2. GW agent exposure paradigm

GW agents used consisted of N,N-diethyl-meta-toluamide (DEET) (100 Maximum Formula, Coleman), which contains 98.1% DEET, permethrin (PER) (Crescent Chemical Co., Inc.), pyridostigmine bromide (PB; TLC Pharmaceutical Standards) and restraint stress to simulate stressors associated with deployment. The combination of PB with DEET or DEET and PER or stress allows for better penetration into CNS [29,30]. We used a chronic exposure paradigm as described for other GWI models [11,31]. These models used routes of administration that are relevant to GW veterans since PB was taken orally and PER and DEET exposure occurred through skin and inhalation [32–34]. At 50–70 d of age mice were randomly assigned to GW exposed or sham-treated control groups. Animals were exposed to PB via oral gavage whereas PER and DEET were applied dermally to a shaved region on the back of the neck. GW groups received PB at 6.5 mg/kg, b.i.d., P.O. (GW1) or 8.7 mg/kg, q.d., P.O. (GW2). The rationale for the PB dosing was described in the accompanying article [124]. Both groups received 1.3 mg/kg PER in 100% DMSO (75 μL/30 g b.w.; topical) and 33% DEET in 70% EtOH (75 μL/30 g b.w.; topical). GW groups were compared to sham (CON) and sham/stress (CON/S) treatment. CON received 0.9% saline (150 μL/30 g, oral gavage) and 70% ETOH (75 μL/30 g b.w., topical) and 100% DMSO (75 μL/30 g b.w., topical). The CON/S group also received 5 min restraint stress in perforated 50 mL conicals once daily [35]. Animals were tested on metabolic, behavioral and exercise parameters as described in the accompanying article [124]. At 195–202 days post treatment (PT), mice were sacrificed under isoflurane anesthesia and blood and brain collected for analysis. Feces were collected at various time points including prior to GW agent exposure (PRE) and

post treatment (PT3, PT188) and used for 16S rRNA next generation sequencing (NGS). A diagram depicting the experimental design and endpoints measured is shown in Fig. 1.

2.3. RT-qPCR analysis of gene markers for neuroinflammation and neuropathic pain

Quantitative PCR (qPCR) was used to study expression of 84 gene biomarkers belonging to the "Mouse Pain: Neuropathic and Inflammatory" panel using the RT^2 Profiler System (Qiagen, PAMM-162ZD-12). At sacrifice (PT199), brains were rapidly hemisected to collect tissue from prefrontal cortex (PFC), hippocampus, hypothalamus and were immediately homogenized in Trizol reagent, snap-frozen in isopentane over a slurry of dry ice and stored at −80 °C until further use. Total RNA was prepared via a modified partial phenol-methanol extraction protocol using the RNeasy Mini Kit (Qiagen, USA). RNA purity, quality and integrity were assessed using a Nanodrop and Bioanalyzer (Agilent 2100, USA). Mean RNA yield was 725 ng/μL (range: 398–1266), mean RNA integrity values (RIN) values were 8.5 (range: 8–9) (Supplementary Information 1, Supplementary Table 1). cDNA was synthesized on a thermal cycler (Biorad) from a 1 μg input RNA per reaction (First Strand kit, Qiagen, USA) according to the manufacturer's instructions, which included genomic DNA digestion. RT-qPCR was carried out on 3–6 biological replicates using the CFX Connect PCR detection system (BioRad, USA). Into each well, master mix, RNA template and nuclease-free H_2O were added for a total of 25 μL/rxn. Amplification reactions for genes of interest were performed in 40 cycles of the following cycling protocol: initial denaturation 95 °C/10 min; per cycle 95 °C/15 s denaturation, 60 °C/60 s (with 1 °C/s ramp rate) primer annealing/extension; 65–95 °C in 0.5 °C, 5 s increments melt curve analysis. Relative expression of genes was normalized to 4 reference genes, whose expression was not affected by treatment (*ActB*, *Gapdh*, *Gusb*, *Hsp90ab1*) and fold-change relative to CON/S or CON was calculated using the delta, delta cycle threshold (Ct) method [36] with the Qiagen GeneGlobe Data Analysis online tool. NCBI GenBank accession numbers are provided in Supplementary Information 1, Supplementary Table 2. Proprietary quality controls (QC) were provided with the following inclusion criteria: mouse genomic DNA contamination (MGDC; if Ct (MGDC) ≥ 35); PCR array reproducibility (PPC; if PPC Ct is ~20 ± 2 and no two arrays have a mean PPC Ct that is >2 Ct away from one another); reverse transcriptase efficiency (RTC; if Delta Ct (AVG RTC - AVG PPC) < 5). One GW2 sample was removed from analysis due to not passing RTC. With a cut-off of Ct = 37, all genes showed detectable expression with the exception of tumor necrosis factor alpha, TNF-a (*Tnfa*), which was excluded from analysis. Heat maps were generated with Prism using fold-change and those showing significant change at $p < .05$ were indicated with an asterisk. Volcano plots of differentially expressed genes (DEGs) were generated using Prism with the cutoff value for up- or down-regulation as ±1.5 and with $p < .05$ of fold change vs control deemed significant. Venn diagrams were created using the free online tool VENNY [37].

2.4. Brain Interleukin-6 ELISA

Whole-brain homogenates were dissociated using RIPA buffer (ThermoScientific) in the presence of protease inhibitors (Complete Protease Inhibitor cocktail; ThermoScientific) followed by centrifugation at 12,000*g* for 20 min at 4 °C. Supernatant was collected and stored at −80 °C until future use. Brain Interleukin-6 (IL-6) was quantified using a commercially available ELISA kit (Cayman Assays, Ann Arbor, MI USA) following

manufacturer's instructions. All samples were normalized for total protein (BCA kit, ThermoScientific).

2.5. GFAP immunohistochemistry

Mice were sacrificed using CO_2 inhalation and perfused transcardially (exsanguinated) with 15 mL 0.01 M phosphate-buffered saline (PBS) followed by 20 mL of 4% paraformaldehyde (PFA) in 0.1 M phosphate buffer. After 24 h post-fix in 4% PFA, brains were cryoprotected in successive incubations of 15 and 30% sucrose in PBS over 3 d. Frozen tissue was cut coronally on a sliding cryostat (Leica Microsystems, Germany) at 40 μm, mounted on gelatinized slides and stored at −80 °C until further use. Subsequently, sections were air-dried at RT for 20 min before being washed extensively in PBS followed by a permeabilization/block step in 4% normal goat serum, 1% bovine serum albumin and 0.3% Triton-X in PBS. Sections were then incubated with a mouse monoclonal anti-GFAP primary antibody conjugated with Cy-3 (1:750; C9205 Sigma Millipore) for 24 h at 4 °C in a humidified chamber with thermoplastic (Parafilm M) coverslips to prevent drying. After washing with PBS, sections were coverslipped with Vectashield Hardset antifade mounting media containing DAPI counterstain (Vector Laboratories, Burlingame, CA).

2.6. Quantitative densitometry

For each animal, images were acquired of 3–6 microscope fields from each hippocampal subfield (CA1, CA3, dentate inner and outer molecular layers and hilus) using a 10× objective on a Zeiss Axioimager M2 microscope equipped with a Hamamatsu ORCA-Flash4.0 V3 digital camera. All images to be compared were acquired using identical microscope settings and were used to quantify GFAP immunoreactive signal using densitometry software (QuPath v0.2.3 [38]). For each sample hippocampal subfield an integrated optical density score was calculated for each designated region of interest (ROI). The integrated optical density (IOD) was calculated as the sum of cell area × mean intensity for each GFAP-positive cell and normalized to total ROI area. Results were reproduced in 3 different experiments containing 2–7 biological replicates per group.

2.7. 16S rRNA gene V4 region sequencing and analysis

DNA from mouse fecal samples was extracted using phenol: chloroform:isoamyl-alcohol (24:24:1, Fisher Scientific) as described previously [39]. The V4 region of bacterial 16S ribosomal RNA genes was amplified as described [40] based on primers for 515F and 806R based on the earth microbiome project [41]. An equal amount of each amplicon was pooled and sequenced on the Illumina MiSeq platform with 2 × 150 paired-end reads. Sequencing reads were then assembled, de-multiplexed, and analyzed using QIIME 1.9.1 [42]. Sequencing results are summarized in Supplementary Information 2, Supplementary Tables 1–2. Redundancy analysis (RDA) was performed using package vegan [43] in R (Supplementary Information 2, Supplementary Table 3).

2.8. Fecal colony plating

Fecal pellets were collected, weighed and immediately suspended in sterile PBS followed by homogenization using a bead beater (BioSpec) at 1400 RPM for 1 min. Homogenates were

serially diluted, pipetted onto LB agar plates and placed in aerobic or anaerobic incubators (37 °C). CFU enumeration of colonies was performed 16–20 h later.

2.9. Plasma endotoxin assay

Blood was collected by cardiac puncture at sacrifice under isoflurane anesthesia. Serum was coagulated for 30 min at RT, followed by separation at 12,000 ×*g* for 20 min under cold centrifugation (4 °C) and stored at −80 °C until further use. A lipopolysaccharide (LPS; 0.5 mg/kg, i.p., sacrificed 6 h later) group served as a positive control. Serum endotoxin levels were analyzed using the Pierce limulus amebocyte lysate (LAL) Chromogenic Endotoxin Quantitation Kit (A39552, ThermoFisher, USA) following the manufacturer's instructions. Standards and samples were prepared in borosilicate glass vials (Globe Scientific Inc.). Sample sera were diluted 1:50 or 1:100 for LPS. The low standard format was utilized for the generation of the standard curve which was used to calculate unknown endotoxin concentrations in Prism. Absorbance was read at 405 nm on a plate reader (iD3, Molecular Devices).

2.10. Intestinal permeability assay

Control and experimental mice were fasted for 15 h overnight (ON) on wood chip bedding. Mice were intragastrically gavaged with 4-kDa dextran conjugated to fluorescein isothiocyanate (FITC) (Sigma-Aldrich; 100 mg/mL) in sterile saline (NaCl, 0.9%) at a single dose (0.6 mg/kg b.w.). After 4 h, mice were euthanized under isoflurane anesthesia and blood (300–400 μL) collected via cardiac puncture into sterile tubes on ice. Supernatant (plasma) was obtained after cold-centrifugation at 10,000 ×*g* for 20 min. Plasma was diluted 1:5 in Milli Q water. Fluorescence was measured spectrophotometrically (GloMax Promega, USA) in 96-well plates (excitation: 490/510–570 nm, 525/580–640 nm). FITC-dextran concentration of samples was determined from a standard curve generated using a diluted fluorophore stock gavage solution in the plasma matrix of fasted untreated mice. Three technical replicates of each sample were run.

2.11. Cultivation of bacterial strains and fecal microbiota transplantation (FMT)

Lactobacillus reuteri (ATCC 23272), was grown anaerobically with deoxygenated de Man, Rogosa & Sharpe (MRS) media or MRS solid agar at 37 °C. MRS (1 L) contained Proteose peptone No.3 10 g; Beef extract 10 g; Yeast extract 5 g; Dextrose 20 g; Glucose 20 g; Tween 80 1 g; K_2HPO_4 2 g; Sodium acetate 5 g; $(NH_4)3$ citrate 2 g; $MgSO_4 \times 7\ H_2O$ 0.10 g; $MnSO_4 \times H_2O$ 0.05 g. Strain identity prior to experimental use was confirmed by 16S amplification and Sanger 16S sequencing. Fecal slurry inoculates were normalized to the equivalent of 300 μL of OD600 = 0.4 culture in MRS broth using quantitative PCR for total 16S using primers 16S-27F [40]. To prepare fecal microbiota transplantations, fecal samples were mechanically disrupted using a bead-beater. The homogenate was centrifuged and pelleted bacteria were resuspended in LYBHI media and used as a gavage solution. LYBHI (1 L) contained BHI Broth 37.00 g; Yeast extract 5 g; Cysteine 1 g; Cellobiose 1 g; Maltose 1 g; Hemin 5 mg.

2.12. Statistical analysis

All statistical analyses were conducted using GraphPad Prism (GraphPad Software, San Diego, CA, USA). All values are expressed as mean ± s.e.m. Student's paired *t*-test was used to compare the effects of exposure. Between group differences were determined using analysis of variance (ANOVA). Where the F ratio was significant, post hoc comparisons were completed using the Tukey's or Dunnet's post hoc test. R (v4.0.4 Boston, MA, USA) was used for analysis of 16S rRNA sequencing data. Group comparisons of community structure were performed using PermaNOVA and Student's t or Mann Whitney tests. F and *p* values are presented in the figure legends or Supplementary Information 1, Statistical Results. Differences were considered statistically significant at $p < .05$.

3. Results

3.1. Two neuroinflammatory transcriptional phenotypes induced by GW agent exposure

In an effort to link the behavioral outcomes of GW agent exposure to neuromolecular events, we investigated the regulation of neuroinflammation/neuropathic genes in PCR array experiments. Proteins encoded by these genes and their pathway designations are shown in Supplementary Information 1, Supplementary Table 3. Exposure-dependent patterns of deregulation were found in homogenates of combined PFC, hippocampus and hypothalamus as compared to CON at PT188 (Fig. 2A). First, we examined the effect of stress alone. There were 7 downregulated DEGs in CON/S, relative to CON (Fig. 2A, B), including *Csf1*, colony stimulating factor 1 of macrophages, *Edn1*, endothelin 1, which is closely associated with neuroinflammation [44], *Faah*, a hydrolase for endocannabinoids and other fatty acid amidated signaling lipids that, when inactivated, produces anti-inflammatory and analgesic actions [45], *Grin1*, the NMDA-type receptor 1 glutamate receptor involved in sensitized pain states, *Kcnq2*, potassium voltage-gated channel subfamily Q member 2, that is inhibited by muscarinic ACh receptors, *Ptger1*, prostaglandin E receptor 1 that contributes to microglial prostaglandin-dependent signaling affecting inflammation and modulation of striatal neurons and which has been implicated in depressive-like and anxiety states [46], *Trpa1*, transient receptor potential cation channel, subfamily A, member 1, a target of endogenous inflammatory agents on nociceptive sensory neurons [47]. The only upregulated gene, *Cck*, cholecystokinin, is associated with peripheral and central pain signaling and plays a role in anxiety and panic disorders [48–50] and may have therapeutic potential for inflammatory bowel disorder [51]. The DEG pattern seen between CON/S relative to CON indicates a complex effect of stress alone on neuroinflammatory and neuropathic pain processes. We also compared GW1 and GW2 to CON. For GW1, DEGs included upregulated expression of *Calca* and *Il6* (Fig. 2E). Therefore, there were no DEGs relative to CON in common between GW1 and CON/S (Fig. 2H). In contrast, GW2 displayed 8 DEGs (downregulated *Cx3cr1*, *Grin2b*, *Pnoc*, *Scn10a* and upregulated *Il1b*, *Pla2g1b*) that were uniquely different (except for *Kcnq2*, *Ptger1*) from DEGs produced by CON/S (Fig. 2F, H), suggesting that GW2 may produce a greater induction of genes including proinflammatory *Il1b* and *Pla2g1b* [52,53].

To determine the sole effects of GW chemical exposure (minus stress) we examined DEGs relative to CON/S. Fig. 2G indicates two dissimilar transcriptional phenotypes in GW1

and GW2 groups. GW1 displayed 5 downregulated DEGs, i.e., *Cck*, *Il1a* (Interleukin-1 alpha, a pro-inflammatory cytokine), *Il2*, a cytokine with complex immunoregulatory function [54], *Ntrk1*, neurotrophic tyrosine kinase receptor 1, and *Penk*, the opioid neurotransmitter preproenkephalin (PENK) expressed in striatum reward pathway [55]. The 7 upregulated DEGs in GW1 were *Adora 1*, adenosine G-protein coupled A1 receptor with proinflammatory actions [56], and *Csf1*, *Edn1*, *Faah*, *Grin1*, *Kcnj6*, the ATP-sensitive potassium inwardly rectifying channel subfamily J member 6 associated with spatial potassium (K+) buffering function of astrocytes and regulation of neuronal activities [57], and *Kcnq2*. The volcano plot in Fig. 2C shows the direction and magnitude of DEGs in GW1 vs. CON/S. Six of the 12 DEGs, *Cck*, *Csf1*, *Edn1*, *Faah*, *Grin1*, *Kcnq2* were also differentially altered in CON vs CON/S (Fig. 2G). The GW2 relative to CON/S comparison in Fig. 2D shows downregulation of *Il10* encoding for the anti-inflammatory cytokine, Interleukin-10 [58], as well as upregulation of 2 pro-inflammatory genes (Fig. 2D). One of these is *Cd4*, a molecule commonly expressed on the surface of T-helper lymphocytes with a recognized critical role in the antigen presentation process and maturation of microglia [59]. The other upregulated DEG, *Edn1*, encodes for endothelin, which triggers reactive microgliosis, regulates IL-6 release, neurotransmission and has been implicated in inflammatory neurological diseases and neurodegeneration [60]. The Venn diagram in Fig. 2G shows that *Edn1* was commonly upregulated in both GW1 and GW2 and CON relative to CON/S. In contrast, *Edn1*, was downregulated in CON/S relative to CON, suggesting that stress drives the change (Fig. 2B, H).

Two different transcriptional phenotypes were produced by GW1 and GW2 dosing regimens relative to CON/S (Fig. 2G). While GW1 had 12 DEGs, GW2 had only 3. These DEG sets are mutually exclusive except for *Edn1* upregulation. Importantly, GW1 showed downregulation of *Il1a*, encoding for the pro-inflammatory cytokine, Interleukin 1*a*, and *Il2*, a gene that encodes for the anti-inflammatory Interleukin 2 (IL2). In contrast, GW2 displayed a downregulated DEG, *Il10*, encoding for the anti-inflammatory cytokine IL-10 and an upregulated pro-inflammatory DEG *Cd4* relative to CON/S. Therefore, the transcriptional phenotype in GW2 may reflect a more specific pro-inflammatory state, while that of GW1 represents a mixed phenotype driven, in part, by stress alone. In order to determine the combined effects of stress and GW agents, we compared all three exposure groups to CON. The Venn diagram in Fig. 2H shows DEGs in GW2 with a prominent pro-inflammatory phenotype including upregulated *Il1b*, *Pla2g1b*. There were no deregulated genes in common between the three treatment groups (Fig. 2H), potentially indicating a unique synergistic effect of GW chemicals and stress in GW2. In summary, the GW2 transcriptional phenotype is characterized by a more specific pro-inflammatory state, i.e., upregulated pro-inflammatory genes (*Cd4*) and downregulated anti-inflammatory genes (*Il10*), that cannot be attributed to an effect of stress alone, while also having a synergistic (plus stress) upregulatory effect on proinflammatory genes *Il1b* and *Pla2g1b*. In comparison, GW1 showed only 1 DEG with proinflammatory actions (*Adora1*) that could not be ascribed to an effect of stress.

The pie chart shown in Fig. 2I indicates the pathways represented by the 22 DEGs (2 genes represent more than one pathway) deregulated by any treatment. Most changes involved genes associated with inflammatory processes (50%), eicosanoid metabolism (8.3%),

glutamate receptors (8.3%), neurotransmitters (8.3%) and potassium channels (8.3%). A smaller fraction of DEGs were associated with either ion channels, sodium channels, purinergic receptors or neurotrophins.

3.2. GW agents produce neuroinflammation: brain IL-6 and astrocyte hypertrophy

Given that DEGs associated with neuroinflammation were upregulated in GW groups (*Adora1*, *Cd4*, *Edn1*, *Il1b* and *Pla2g1b*), we examined the expression of IL-6 in brain lysates since it is a major pro-inflammatory cytokine having pleiotropic properties with opposite roles to IL-2 and IL-10 [61,62] and an important modulator of CD4 T cell effector functions [63]. Also, both GW1 and GW2 displayed upregulation of *Edn1*, a gene that encodes for endothelin which regulates circulating IL-6 depending on its levels [60]. We found that mean brain IL-6 levels were significantly greater in GW2 but not GW1 relative to CON/S ($p < .05$) confirming that only the PB dosing in GW2 produced persistent neuroinflammation that was evident at 199 days post treatment (Fig. 3).

Cytokines such as IL-6 are potent regulators of astrogliosis, which contribute directly to the pathogenesis of CNS injury [64,65]. Therefore, we compared the density of glial fibrillary acidic protein (GFAP), a marker of astrocytes, in GW vs control groups. Fig. 4 shows representative micrographs of GFAP immunohistochemical results from each group. Intense profiles of hypertrophied astrocytes were seen in CA1 stratum oriens and stratum radiatum of GW1 and GW2 as compared to CON/S (Fig. 4A–D). When computer-assisted densitometric data were pooled and quantified, a significant increase in GFAP immunoreactive density was measured in CA1 subfields of GW1 and GW2 groups vs CON/S ($p < .05$, Fig. 4E). In contrast, group differences in GFAP immunoreactivity (ir) were not obvious in the dentate gyrus (Fig. 4F–J), hilus or CA3 (not shown).

3.3. Different gut microbiome community structure in GW1 and GW2

We hypothesized that differential gut microbiome changes accompany the two GW phenotypes characterized according to cognition, exercise fatigue and neuroinflammatory profile. To determine if the community of commensal microorganisms of the gastrointestinal tract was being modified by our experimental treatments, we performed sequencing of bacterial 16S ribosomal RNA in fecal samples of CON, CON/S, GW2, GW1 mice collected at pre-exposure, PT 3 and PT188. We observed no major differences in alpha diversity across this dataset (Supplementary Information 1, Supplementary Fig. 2). To examine overall community structure distances, we used principal coordinate analysis (PCoA) of weighted Unifrac distances between gut microbiomes (Fig. 5A–D). Weighted Unifrac is a distance metric that describes the relatedness of different microbial communities, incorporating measures of the phylogenetic distance between observed microorganisms and their relative abundance in different communities. Briefly, a phylogenetic tree is constructed incorporating all 16S sequences of observed microbial taxa and then used to calculate the summed shared branch length of microbial communities based on their microbial content, adjusted for the relative abundance of individual taxa in each community. Beta-diversity PCoA using weighted Unifrac revealed that gut microbial communities changed with the initiation of exposure in all treatment groups (Fig. 5A–C), with separation evident along the primary axis of variation (PC1–38.6%) between samples at pre- and PT188, likely driven

by stress but significant only in GW2 ($P < .05$; Fig. 5A). We performed a PermaNOVA analysis that revealed significant differences in overall community structure. Between-group comparisons of community variation at PT188 indicated a significant difference in the effect of CON/S and GW1 ($P < .05$) or GW2 exposure ($P < .0001$) (Fig. 5D). Changes due to GW1 and GW2 exposures, compared to pre-treatment baseline, produced different weighted Unifrac distance as compared to changes resulting from CON/S, indicating a significant effect of GW1 exposure on gut dysbiosis (Fig. 5D). When enumerating fecal colonies grown on agar plates in aerobic and anaerobic conditions from our experimental groups, we observed changes in the quantity of aerobic colonies at PT3 in both GW groups, while stress drove an increase in anaerobic colonies (Supplementary Information 1, Supplementary Fig. 1).

We then employed Redundancy Analysis (RDA) to correlate microbial taxa to treatment group in order to identify specific microbial contributors to these overall community differences (Fig. 5E, Supplementary Information 2, Supplementary Table 3). This analysis examines the relationships between individual microbial taxa and community structure. As pre-treatment communities were similar and differences began to be observed at PT3, we focused on group differences at this time-point induced by CON/S and exposure to GW2, versus the pre-treatment fecal microbiome. We observed that higher abundance of bacteria in genus Lactobacillus most strongly characterized the CON/S group and that Bacteroidales in family S24–7 was most strongly associated with GW2. The results of PCoA and RDA indicated different gut microbial communities in GW1 and GW2. Interestingly, an unidentified taxon in Lachnospiraceae, a family of anaerobic bacteria in the order Clostridiales, was associated by RDA with gut commensal communities prior to treatment with GW agents. This taxon decreased significantly with exposure to GW2 at PT3 ($P < .001$), a reduction that was maintained out to PT 188 ($P < .05$; Fig. 5F). Similar results were obtained for GW1 at PT188 ($P < .05$; data not shown).

3.4. GW agent exposure produces endotoxemia and Lactobacillus reuteri supplementation provides better gut barrier function that FMT from GW mice

We further hypothesized that the altered microbiome seen in GW mice may be associated with an overabundance in blood levels of LPS, which may provide an environment conducive to chronic inflammation. Results of LAL endotoxin assay showed significant elevation in systemic endotoxemia in GW1 and GW2 relative to CON/S ($p < .05$ and $p < .001$, Fig. 6A). However, this effect was mild as compared to mice treated with a low dose of LPS ($p < .0001$, 0.5 mg/kg; i.p.). Because the gut microbiome results indicated that Lactobacillus is preferentially associated with CON/S as compared to GW groups, we examined the effects of *Lactobacillus reuteri* ATCC 23272 supplementation, a species with known gut barrier promoting effects [66,67], by administering *L. reuteri* to germ-free mice. Gut barrier function was measured physiologically using a FITC-dextran assay. Fig. 6B shows that mice receiving *L. reuteri* engraftment display significantly less gut permeability than mice receiving a microbiota transplantation using feces of GW2 mice and collected at PT 188.

3.5. Summary of GW1 and GW2 phenotypic changes and biomarkers

Table 1 shows the summary of GW1 and GW2 biomarkers obtained for gut dysbiosis, systemic endotoxemia, and neuroinflammation from the current study alongside phenotypic characteristics obtained on the same mice and reported in the accompanying manuscript [124]. The latter were classified according to a subset of the symptom groups included in the Kansas case definition [23]: neurological/cognitive/mood, fatigue, pain as well as other symptoms such as metabolic (insulin insensitivity, body weight, lean/fat mass), sensorimotor and locomotion ability.

4. Discussion

In an accompanying article in this issue of *Life Sciences*, we describe persistent and delayed cognitive/mood disturbances and exercise intolerance produced by chronic GW agent exposures in a mouse model of GWI [124], resembling the cognitive decline and memory loss and chronic fatigue seen in GWVs [68]. The present study describes the GW agent-induced changes in neuroinflammatory markers, gut microbiome and systemic endotoxemia, occurring in tandem with these phenotypes. Two different cognitive/fatigue phenotypes were described for GW1 and GW2, receiving different PB exposures. GW1 was characterized by deficient avoidance learning/memory and long-term novel object recognition memory and behavioral despair, while GW2 showed pronounced impairment in avoidance learning and memory, exaggerated exercise fatigue and glucose metabolic alterations. These phenotypes also differed on the basis of neuromolecular correlates described in this study. Importantly, the neuromolecular profiles reported here were characterized at more than 6 months after exposure suggesting persistent changes in neuroinflammatory state promoted by GW chemicals.

We speculate that the two different PB dosing regimens had differential effects on cholinergic signaling, which governs GWI domains (e.g. muscle function, associative learning and memory, sleep) [69,70] via muscarinic and nicotinic ACh receptors (AChRs) [71]. When applied acutely, PB, like sarin gas, blocks acetylcholinesterase (AChE), the enzyme which degrades ACh, leading to its accumulation at ACh receptors and overstimulation of the cholinergic system. However, *chronic* (15-day) exposure to PB alone, or in combination with DEET or DEET/PER, results in increased AChR levels of muscarinic and nicotinic ACh receptors in rat cortex [29], in tandem with reduced performance on beam walking. Therefore, upregulation of AChR density is likely accompanied by other opposing changes [29]. Downregulation of muscarinic AChRs after prolonged exposure to another AChEI, sarin, has also been shown [72]. Reduced cholinergic signaling can also be produced by desensitization and inactivation of AChRs after prolonged AChE inhibition [73,74]. Receptor desensitization due to prolonged activation of muscarinic receptors has been implicated as the root cause for inhibition of hippocampal LTP induction [75], the cellular manifestation of associative learning [76]. Additionally, low level PB can alter transcription of AChE, depressing cholinergic function [77,78]. In GW1, which was administered PB twice daily, cholinergic receptors were likely more saturated due to a more continuous elevation of ACh due to acetylcholinesterase inhibition (AChEI) than that experienced in GW2. Using similar twice daily administration of PB, others have shown increased

tolerance of muscarinic AChR signaling [79] and muscarinic receptor-mediated apoptosis of cortical and hippocampal neurons [80]. These complex pharmacological properties of the central and peripheral cholinergic systems make it difficult to pinpoint the molecular mechanisms associated with GW1 relative to GW2, until additional pharmacological studies are conducted.

Persistent GW1 and GW2 phenotypes, which show cognitive, mood and fatigue alterations may be associated with neuroinflammation. For example, mood disorders, alongside cognitive deficits and fatigue, are commonly accompanied by neuroinflammation in humans and experimental rodents [22,81–83]. Results from PCR array identified DEGs with pro- and anti-inflammatory actions, indicating that GW agents influence the brain's innate immune response. Importantly, two distinct neuroinflammatory transcriptional phenotypes were identified for GW1 and GW2. The GW2 transcriptional phenotype was characterized by a more specific pro-inflammatory state, i.e., upregulated pro-inflammatory gene (*Cd4*) and downregulated anti-inflammatory gene (*Il10*), that cannot be attributed to an effect of stress alone. In addition, GW2 also appeared to have a synergistic (plus stress) upregulatory effect on proinflammatory genes *Il1b* and *Pla2g1b*. In comparison, GW1 showed only 1 DEG with proinflammatory actions (*Adora1*) that could not be ascribed to an effect of stress. Both GW1 and GW2 DEG sets (compared to CON/S) share an upregulated DEG, *Edn1*, encoding for endothelin which triggers reactive microgliosis and regulates IL-6 release [60]. These findings suggest that unlike GW1, GW2 was represented by a signature exclusively promoting neuroinflammation. The DEG signature in GW2 may underlie the exclusive GW2 phenotype characterized by combined cognitive impairment, fatigue and insulin resistance (see Table 1).

Since morphological signs of chronic inflammation in GW animal models (using PB/PER/DEET) include hypertrophied astrocytes and partial loss of neurons in hippocampal subfields [7,29,84,85], we next examined the effect of GW agents on astrogliosis in the hippocampus using the astrocytic marker GFAP. Both GW groups showed GFAP-positive astrocyte hypertrophy in CA1 subfield, which may explain the deficient avoidance learning seen in both GW groups due to its contribution in regulating fear-motivated associative learning [86]. In addition, altered NOR memory is dependent on several brain regions and neurotransmitter systems, including the hippocampus and perirhinal regions [87–89]. An exacerbated central inflammatory state involving activated astrocytes and microglia has also been characterized in ill GWVs [17], represented by cortical upregulation of mitochondrial translocator protein (TSPO), defined as a marker of microglial activity, astrogliosis and by severity of neuroinflammation in autoimmune diseases [90]. This type of neuropathology may underlie reduced MRI volume, altered white matter microstructural integrity and altered PFC activity found in association with impaired cognitive functioning or chronic fatigue complaints in GWVs exposed to Gulf War chemicals [2,91–93].

Reactive astrocytes can produce the major inflammatory cytokine mediating the innate inflammatory response, IL-6, as well as others, IL-1β, TNF-α, INF-γ, transforming growth factor beta (TGF-β) [94]. Examination of brain levels of IL-6 showed that only GW2 displayed upregulated levels in whole brain homogenates. In support of our findings, a previous report has shown dysregulation of genes encoding IL-6 and IL-1ß, in ventral

hippocampus of rodents produced by exposure to combinations of Gulf War chemicals PB/PER and/or PER/DEET/CORT/DFP [15]. A 10-day exposure to sarin in heat stress conditions has also been reported to increase mRNA for brain IL-6 and IL-1ß, TNF-α in rats [72]. Elevated levels of IL-6 in only GW2 appear to conflict with our results showing upregulated GFAP immunoreactivity in both GW1 and GW2. However, the latter is representative of the hippocampus only, whereas IL-6 samples were pooled from various brain regions. Additionally, IL-6 levels can also be produced by activated microglia which is likely in GW2 since, relative to CON/S, only this group displayed upregulated *Cd4*, an immunological marker expressed on the surface of resident microglia [95]. Our DEG and IL-6 characterization is in agreement with reports of significant/apparent increases in serum IL-6 and elevated levels of IL-1β in ill GWVs [4,18,21]. Ill GWVs show decreased hippocampal volume as part of their inflammatory state indicated by elevated systemic levels of C-Reactive protein, produced by the liver in response to inflammation [96].

Taken together, our data showing pro-inflammatory DEG profile, upregulated hippocampal GFAP immunoreactivity, and brain IL-6 production indicate that the response to GW agents, especially GW2, likely involves an intensified neuroinflammatory pathology that is persistent at >6 months post exposure to GW chemicals. Activated astrocytes express additional proinflammatory mediators, such as NF-κB [97,98] and, like microglia, astrocytes can produce cytokines and chemokines, such as IL-6, type I and II Interferons (IFNs), and TNF, contributing to the amplification of neuroinflammation [99,100]. Other reports have shown similar changes in these endpoints, as well as increased expression of TLR4 and TNF-α subsequent to GW agent exposure [26]. With regard to IL-6, elevated brain levels are thought to contribute to dementia [101], and neurodegenerative disease phenotypes [102], which may possibly have relevance to a variety of neurological disorders (ALS, stroke, migraine headaches) that occur at higher rates in GWVs [2]. For example, elevated TSPO positron emission tomography (PET) ligand binding, reported in brain imaging studies of ill GWVs, has also been predictably demonstrated across a broad spectrum of neurodegenerative diseases in disease-relevant brain areas [103].

In further support of our findings, chronic symptoms in GWI are reported to occur in combination with intensified neuroinflammatory responses in animal studies [4,5,7]. These findings in animals mimic several pathological alterations in GWVs such that symptom severity has been associated with intensified neuroinflammatory responses [4,104]. For example, higher fatigue severity days were associated with greater IL-1β in ill GWVs relative to healthy veteran controls [19]. Greater fatigue has been reported by ill GWVs during exercise (30-min cycling at 70% heart rate reserve) as compared to healthy veterans [105]. Moreover, symptom severity in GWI veterans after maximal graded exercise challenge is correlated with immune pathway activity, such as serum alterations in nuclear factor kappa beta (NF-κB) pathway (transcription factor regulating innate immunity) and IL-10, and abundance of Cd2-positive cell (T and natural killer lymphocytes) [21]. Moreover, worse outcomes on self-reported symptom measures for fatigue and sleep functioning in GWVs are correlated with upward trending levels of serum IL-6, TNF receptor type I and II and widespread microstructural changes in the frontal and limbic regions [21].

The results of PCoA and RDA using fecal 16S rRNA gene sequencing data indicated different gut microbial communities in GW1 and GW2. PCoA analysis shows that gut microbiome structure changes were predominantly caused by exposure to GW2 when compared to CON/S. Treatment with GW1 or GW2 showed significantly different effect on weighted Unifrac distance than did CON/S indicating meaningful changes in community structure were produced by chronic exposure to GW agents. These results were evident at PT 188 indicating durable modification of gut microbiome by GW exposure. Several bacterial taxa were associated with changes in overall community structure, with different profiles in GW1 and GW2. RDA results showed that Bacteroidales family S24–7 was most associated with GW2 and Lactobacillus with CON/S, evident at 3 days post exposure. The relative depletion in GW groups of Lactobacillus, which facilitate production of short-chain fatty acids (SCFAs), preservation of barrier function and reduce central inflammation [106,107], has been noted previously after acute GW treatment to mice [25]. In addition, there was a depletion in the relative abundance of a member of family Lachnospiraceae after GW1 and GW2 exposure. This community structural change is observed as early as 3 days post treatment, but differences are maintained out to 188 days post treatment. In support of our findings, a recent report by Bose and colleagues [28] showed that GW agents (2 mg/kg PB, 200 mg/kg PER, tri-weekly for 2 wk) produce significant depletion of Lachnospiraceae at 5 months post-GW chemical exposure [28]. Members of family Lachnospiraceae are important producers of the SCFA butyrate [108,109], and are associated with maintenance of gut barrier function [110,111]. Since butyrate has been shown to ameliorate intestinal and inflammatory processes in GWI mice [25] and neuroinflammation [112], the microbiome structure changes we observed in GW mice suggest a compromised gut barrier and possible route leading to neuroinflammation in GW mice. Interestingly, Alhasson and colleagues [26] reported a decrease in abundance of family-level OTU S24–7 (Bacteroidales family) and greater abundance of two unclassified/unnamed families from the order Clostridiales and in their GW chemical exposed relative to unexposed group [26]. Our discrepant results may be due to the chronic nature of the GW agent exposure (28 d) used here as compared to the acute exposure (tri-weekly for 1 week) of GW agents plus ip corticosterone treatment used in the previous study [26].

GW-induced changes in microbiome community structure as well as neuroinflammatory phenotypes occurred concomitant with systemic endotoxemia, suggesting a probable involvement of gut-brain interaction in the neuropathology. Production of IL-6 may be triggered downstream from LPS transfer from the gut which can initiate the innate inflammatory response [94]. In particular, transfer of intestinal content including LPS-rich (endotoxin) gram-negative bacteria (notably members of phyla Bacteroidetes) into the systemic circulation [113] is associated with increased production of pro-inflammatory cytokines and reactive oxygen species. LPS enters the brain via transporters [114] or by penetration of the blood brain barrier shown to be compromised after chronic exposure to GW agents [11]. We speculate that significant differences in the gut microbiome arise from exposure to GW chemicals/stress, and via systemic endotoxemia [115] and may produce neuroinflammation [15,85,116] via a gut-brain pathway leading to cognitive and fatigue phenotypes. Thus, either a disrupted intestinal barrier function or a vagally-mediated mechanism [117] may link gut microbiome alterations, neuroinflammation and impaired

physiology in GWI. While there is some evidence for this possibility further study is needed [26]. Indeed, gut dysbiosis and changes in microbe-derived molecules in host blood have been shown to influence cerebral signaling molecules and cognitive function [118]. If corroborated in future studies, possible gut-brain interactions may represent a promising target for future mechanistic studies on GWI pathophysiology as well as probiotic therapies [119–122].

To determine the effects of supplementation with Lactobacillus on gut permeability we colonized germ-free mice with *Lactobacillus reuteri* and compared it to that of germ free mice with engrafted FMT obtained from GW2 mice. Past studies report that *L. reuteri* ATCC 23272 is associated with improved gut function [66,67], as well as improved cognitive ability [123]. Germ-free mice receiving GW2 FMT showed significantly greater gut permeability than control mice receiving *L. reuteri* transplants. These results support the possibility that probiotic therapy with *L. reuteri* may improve gut barrier function in mice exposed to GW2, although additional studies are needed to confirm this. These findings are relevant for planning future safe and effective probiotic therapies to alleviate symptoms in our GWI veterans.

Supplementary Material

Refer to Web version on PubMed Central for supplementary material.

Acknowledgements

We acknowledge technical assistance from S. Sriram, UC Riverside Neuroscience Graduate Program, Drs M. Collin and H. Clark at Institute for Integrative Genome Biology Genomics Core, UC Riverside. We thank Drs. I. Ethell, F. Sladek, S. Tiwari-Woodruff for breeder mice. We are grateful to Drs. P. Deol and F. Sladek for comments on PCR data analysis. We are grateful to Dr. M. Nair for gift of LPS plasma. Images were created using BioRender.com.

Funding

GWIRP Department of Defense W81XWH-19-1-0802 (to M.C.C and N.I.z.N.), UC Riverside GRMP (E.V.K.), UC Riverside Mini Grant (A.E. B.), Sigma Xi Honors Research Society GIAR (A.E.B.); American Physiological Society STRIDE Fellowship (to A.E.B.), National Institute of General Medical Sciences R35GM124724, National Institutes of Health NIAID grants R01AI157106 (to A.H.) and National Institutes of Health grants 2R01DK091281, 1R01AI153314, 1R01DK130373, R21AI152017 (to D.F.M.)

Abbreviations:

ACh	acetylcholine
AChE	acetylcholinesterase
AChEI	acetylcholinesterase inhibitor
b.i.d.	*bis in die* - twice daily
CFU	colony forming unit
CNS	central nervous system
CON	sham group

CON/S	sham and stress group
DEET	N,N-diethyl-meta-toluamide
DEGs	differentially expressed genes
DG Mol	dentate gyrus molecular layer
DMSO	dimethyl sulfoxide
EtOH	ethanol
FITC	fluorescein isothiocyanate
FMT	fecal microbiota transplantation
GFAP	glial fibrillary acidic protein
GWI	Gulf War Illness
GWVs	Gulf War veterans
IL-6	interleukin 6
IL-10	interleukin 10
INF-γ	interferon gamma
IOD	integrated optical density
LAL	limulus amebocyte lysate
LB	Luria broth
LPS	lipopolysaccharide
LYBHI	Brain Heart Infusion medium
MRS	de Man, Rogosa & Sharpe medium
NF-κB	nuclear factor kappa beta
OTU	operational taxonomic unit
PB	pyridostigmine bromide
PCoA	principal coordinate analysis
PER	permethrin
PFC	prefrontal cortex
P.O.	*per os* - by mouth
PT	post-treatment day
q.d.	*quaque die* - once daily

RDA	redundancy analysis
ROI	region of interest
RT-qPCR	reverse transcriptase quantitative PCR
rRNA	ribosomal RNA
SCFA	short-chain fatty acid
SO	stratum oriens
SR	stratum radiatum
TNF	tumor necrosis factor
TGF-β	Transforming growth factor beta
TSPO	translocator protein

References

[1]. Golomb BA, Acetylcholinesterase inhibitors and gulf war illnesses, Proc. Natl. Acad. Sci. U. S. A. 105 (2008) 4295–4300, 10.1073/pnas.0711986105. [PubMed: 18332428]

[2]. White RF, Steele L, O'Callaghan JP, Sullivan K, Binns JH, Golomb BA, Bloom FE, Bunker JA, Crawford F, Graves JC, Hardie A, Klimas N, Knox M, Meggs WJ, Melling J, Philbert MA, Grashow R, Recent research on Gulf War illness and other health problems in veterans of the 1991 Gulf War: effects of toxicant exposures during deployment, Cortex 74 (2016) 449–475, 10.1016/j.cortex.2015.08.022. [PubMed: 26493934]

[3]. United States Department of Veterans Affairs, Research Advisory Committee on Gulf War Veterans' Illnesses, Gulf War Illness and the Health of Gulf War Veterans: Scientific Findings and Recommendations, U.S. Government Printing Office, 2008. https://play.google.com/store/books/details?id=IJ_CrkE1jdgC.

[4]. Abou-Donia MB, Conboy LA, Kokkotou E, Jacobson E, Elmasry EM, Elkafrawy P, Neely M, 'dale'Bass CR, Sullivan K, Screening for novel central nervous system biomarkers in veterans with Gulf War illness, Neurotoxicol. Teratol 61 (2017) 36–46, 10.1016/j.ntt.2017.03.002. [PubMed: 28286177]

[5]. Dickey B, Madhu LN, Shetty AK, Gulf War illness: mechanisms underlying brain dysfunction and promising therapeutic strategies, Pharmacol. Ther. 220 (2021), 107716, 10.1016/j.pharmthera.2020.107716. [PubMed: 33164782]

[6]. Sullivan K, Krengel M, Proctor SP, Devine S, Heeren T, White RF, Cognitive functioning in treatment-seeking Gulf War veterans: pyridostigmine bromide use and PTSD, J. Psychopathol. Behav. Assess. 25 (2003) 95–103, 10.1023/A:1023342915425.

[7]. Parihar VK, Hattiangady B, Shuai B, Shetty AK, Mood and memory deficits in a model of Gulf War illness are linked with reduced neurogenesis, partial neuron loss, and mild inflammation in the hippocampus, Neuropsychopharmacology 38 (2013) 2348–2362, 10.1038/npp.2013.158. [PubMed: 23807240]

[8]. Ramirez-Sanchez I, Navarrete-Yañez V, Garate-Carrillo A, Loredo M, Lira-Romero E, Estrada-Mena J, Campeau A, Gonzalez D, Carrillo-Terrazas M, Moreno-Ulloa A, Ceballos G, Villarreal F, Development of muscle atrophy and loss of function in a Gulf-War illness model: underlying mechanisms, Sci. Rep. 10 (2020) 14526, 10.1038/s41598-020-71486-w. [PubMed: 32884027]

[9]. Abou-Donia MB, Wilmarth KR, Jensen KF, Oehme FW, Kurt TL, Neurotoxicity resulting from coexposure to pyridostigmine bromide, deet, and permethrin: implications of Gulf War chemical exposures, J. Toxicol. Environ. Health 48 (1996) 35–56, 10.1080/009841096161456. [PubMed: 8637057]

[10]. Abou-Donia MB, Wilmarth KR, Abdel-Rahman AA, Jensen KF, Oehme FW, Kurt TL, Increased neurotoxicity following concurrent exposure to pyridostigmine bromide, DEET, and chlorpyrifos, Fundam. Appl. Toxicol. 34 (1996) 201–222, 10.1006/faat.1996.0190. [PubMed: 8954750]

[11]. Abdel-Rahman A, Shetty AK, Abou-Donia MB, Disruption of the blood-brain barrier and neuronal cell death in cingulate cortex, dentate gyrus, thalamus, and hypothalamus in a rat model of Gulf-War syndrome, Neurobiol. Dis. 10 (2002) 306–326. [PubMed: 12270692]

[12]. Kodali M, Hattiangady B, Shetty GA, Bates A, Shuai B, Shetty AK, Brain Behav. Immun. 69 (2018) 499–514, 10.1016/j.bbi.2018.01.009. [PubMed: 29454881]

[13]. O'Callaghan JP, Kelly KA, Locker AR, Miller DB, Lasley SM, J. Neurochem. 133 (2015) 708–721, 10.1111/jnc.13088. [PubMed: 25753028]

[14]. Johnson GJ, Slater BCS, Leis LA, Rector TS, Bach RR, Blood biomarkers of chronic inflammation in Gulf War illness 11 (2016), e0157855, 10.1371/journal.pone.0157855.

[15]. Carpenter JM, Gordon HE, Ludwig HD, Wagner JJ, Harn DA, Norberg T, Filipov NM, Neurochemical and neuroinflammatory perturbations in two Gulf War illness models: modulation by the immunotherapeutic LNFPIII 77 (2020) 40–50, 10.1016/j.neuro.2019.12.012.

[16]. Hossain MM, Liu J, Richardson JR, Pyrethroid insecticides directly activate microglia through interaction with voltage-gated sodium channels, Toxicol. Sci. 155 (2017) 112–123, 10.1093/toxsci/kfw187. [PubMed: 27655349]

[17]. Alshelh Z, Albrecht DS, Bergan C, Akeju O, Clauw DJ, Conboy L, Edwards RR, Kim M, Lee YC, Protsenko E, Napadow V, Sullivan K, Loggia ML, Brain Behav. Immun. 87 (2020) 498–507, 10.1016/j.bbi.2020.01.020. [PubMed: 32027960]

[18]. Butterick TA, Trembley JH, Hocum Stone LL, Muller CJ, Rudquist RR, Bach RR, Gulf War illness-associated increases in blood levels of interleukin 6 and C-reactive protein: biomarker evidence of inflammation, BMC Res.Notes 12 (2019) 816, 10.1186/s13104-019-4855-2. [PubMed: 31852524]

[19]. Parkitny L, Middleton S, Baker K, Younger J, Evidence for abnormal cytokine expression in gulf war illness: a preliminary analysis of daily immune monitoring data, BMC Immunol. 16 (2015) 57, 10.1186/s12865-015-0122-z. [PubMed: 26420016]

[20]. Georgopoulos AP, James LM, Carpenter AF, Engdahl BE, Leuthold AC, Lewis SM, Gulf War illness (GWI) as a neuroimmune disease, Exp. Brain Res. 235 (2017) 3217–3225, 10.1007/s00221-017-5050-0. [PubMed: 28762055]

[21]. Broderick G, Ben-Hamo R, Vashishtha S, Efroni S, Nathanson L, Barnes Z, Fletcher MA, Klimas N, Altered immune pathway activity under exercise challenge in Gulf War illness: an exploratory analysis, Brain Behav. Immun. 28 (2013) 159–169, 10.1016/j.bbi.2012.11.007. [PubMed: 23201588]

[22]. Trageser KJ, Sebastian-Valverde M, Naughton SX, Pasinetti GM, The innate immune system and inflammatory priming: potential mechanistic factors in mood disorders and Gulf War illnessFront. Psychiatry. 11 (2020) 704, 10.3389/fpsyt.2020.00704.

[23]. Steele L, Prevalence and patterns of Gulf War illness in Kansas veterans: association of symptoms with characteristics of person, place, and time of military service, Am. J. Epidemiol. 152 (2000) 992–1002, 10.1093/aje/152.10.992. [PubMed: 11092441]

[24]. Institute of Medicine, Board on the Health of Select Populations, Committee on Gulf War and Health: Treatment for Chronic Multisymptom Illness, Gulf War and Health: Treatment for Chronic Multisymptom Illness, National Academies Press, 2013, 10.17226/13539.

[25]. Seth RK, Kimono D, Alhasson F, Sarkar S, Albadrani M, Lasley SK, Horner R, Janulewicz P, Nagarkatti M, Nagarkatti P, Sullivan K, Chatterjee S, Toxicol. Appl. Pharmacol. 350 (2018) 64–77, 10.1016/j.taap.2018.05.006. [PubMed: 29751049]

[26]. Alhasson F, Das S, Seth R, Dattaroy D, Chandrashekaran V, Ryan CN, Chan LS, Testerman T, Burch J, Hofseth LJ, Horner R, Nagarkatti M, Nagarkatti P, Lasley SM, Chatterjee S, Altered gut microbiome in a mouse model of Gulf War illness causes neuroinflammation and intestinal injury via leaky gut and TLR4 activation 12 (2017), e0172914, 10.1371/journal.pone.0172914.

[27]. Janulewicz PA, Seth RK, Carlson JM, Ajama J, Quinn E, Heeren T, Klimas N, Lasley SM, Horner RD, Sullivan K, Chatterjee S, The gut-microbiome in Gulf War veterans: a preliminary report, Int. J. Environ. Res. Public Health 16 (2019), 10.3390/ijerph16193751.

[28]. Bose D, Saha P, Mondal A, Fanelli B, Seth RK, Janulewicz P, Sullivan K, Lasley S, Horner R, Colwell RR, Shetty AK, Klimas N, Chatterjee S, Obesity worsens Gulf War illness symptom persistence pathology by linking altered gut microbiome species to long-term gastrointestinal hepatic, and neuronal inflammation in a mouse model 12 (2020) 2764, 10.3390/nu12092764.

[29]. Abou-Donia MB, Dechkovskaia AM, Goldstein LB, Abdel-Rahman A, Bullman SL, Khan WA, Co-exposure to pyridostigmine bromide, DEET, and/or permethrin causes sensorimotor deficit and alterations in brain acetylcholinesterase activity, Pharmacol. Biochem. Behav. 77 (2004) 253–262, 10.1016/j.pbb.2003.10.018. [PubMed: 14751452]

[30]. Friedman A, Kaufer D, Shemer J, Hendler I, Soreq H, Tur-Kaspa I, Pyridostigmine brain penetration under stress enhances neuronal excitability and induces early immediate transcriptional response, Nat. Med. 2 (1996) 1382–1385, 10.1038/nm1296-1382. [PubMed: 8946841]

[31]. Carreras I, Aytan N, Mellott T, Choi J-K, Lehar M, Crabtree L, Leite-Morris K, Jenkins BG, Blusztajn JK, Dedeoglu A, Anxiety, neuroinflammation, cholinergic and GABAergic abnormalities are early markers of Gulf War illness in a mouse model of the disease, Brain Res. 1681 (2018) 34–43, 10.1016/j.brainres.2017.12.030. [PubMed: 29277710]

[32]. Institute of Medicine, Board on the Health of Select Populations, Committee on Gulf War and Health: Health Effects of Serving in the Gulf War, Update 2009, Gulf War and Health: Volume 8: Update of Health Effects of Serving in the Gulf War, National Academies Press, 2010. https://play.google.com/store/books/details?id=dzJkAgAAQBAJ.

[33]. Mawson AR, Croft AM, Int. J. Environ. Res. Public Health 16 (2019), 10.3390/ijerph16010111.

[34]. R.A.C. on Gulf War Veterans' Illnesses, Gulf War Illness and the Health of Gulf War Veterans: Research Update and Recommendations, 2009–2013, US Government Printing Office, 2014.

[35]. Parihar VK, Hattiangady B, Kuruba R, Shuai B, Shetty AK, Predictable chronic mild stress improves mood, hippocampal neurogenesis and memory, Mol. Psychiatry 16 (2011) 171–183, 10.1038/mp.2009.130. [PubMed: 20010892]

[36]. Livak KJ, Schmittgen TD, Analysis of relative gene expression data using real-time quantitative PCR and the 2(-Delta Delta C(T)) method, Methods 25 (2001) 402–408, 10.1006/meth.2001.1262. [PubMed: 11846609]

[37]. Oliveros JC, VENNY. An interactive tool for comparing lists with Venn diagrams, https://ci.nii.ac.jp/naid/20001505977/, http://bioinfogp.cnb.csic.es/tools/venny/index.html, 2007. (Accessed 26 October 2021).

[38]. Bankhead P, Loughrey MB, Fernández JA, Dombrowski Y, McArt DG, Dunne PD, McQuaid S, Gray RT, Murray LJ, Coleman HG, James JA, Salto-Tellez M, Hamilton PW, QuPath: open source software for digital pathology image analysis, Sci. Rep. 7 (2017) 16878, 10.1038/s41598-017-17204-5. [PubMed: 29203879]

[39]. Hsiao A, Ahmed AMS, Subramanian S, Griffin NW, Drewry LL, Petri WA Jr., R. Haque, T. Ahmed, J.I. Gordon, Members of the human gut microbiota involved in recovery from Vibrio cholerae infection, Nature 515 (2014) 423–426, 10.1038/nature13738. [PubMed: 25231861]

[40]. Alavi S, Mitchell JD, Cho JY, Liu R, Macbeth JC, Hsiao A, Interpersonal gut microbiome variation drives susceptibility and resistance to cholera infection, Cell 181 (2020) 1533–1546.e13, 10.1016/j.cell.2020.05.036. [PubMed: 32631492]

[41]. 16S Illumina Amplicon Protocol: Earth Microbiome Project (n.d.), https://earthmicrobiome.org/protocols-and-standards/16s/. (Accessed 28 February 2021).

[42]. Caporaso JG, Kuczynski J, Stombaugh J, Bittinger K, Bushman FD, Costello EK, Fierer N, Peña AG, Goodrich JK, Gordon JI, Huttley GA, Kelley ST, Knights D, Koenig JE, Ley RE, Lozupone CA, McDonald D, Muegge BD, Pirrung M, Reeder J, Sevinsky JR, Turnbaugh PJ, Walters WA, Widmann J, Yatsunenko T, Zaneveld J, Knight R, QIIME allows analysis of high-throughput community sequencing data, Nat. Methods 7 (2010) 335–336, 10.1038/nmeth.f.303. [PubMed: 20383131]

[43]. Oksanen J, Blanchet G, Friendly M, Kindt R, Legendre P, McGlinn D, Minchin PR, O'Hara RB, Simpson GL, Solymos P, Vegan: Community Ecology Package. R Package Version 2.5–4, 2020 (n.d.).

[44]. D'Orléans-Juste P, Akide Ndunge OB, Desbiens L, Tanowitz HB, Desruisseaux MS, Endothelins in inflammatory neurological diseases, Pharmacol. Ther. 194 (2019) 145–160, 10.1016/j.pharmthera.2018.10.001. [PubMed: 30291906]

[45]. Ahn K, Johnson DS, Cravatt BF, Fatty acid amide hydrolase as a potential therapeutic target for the treatment of pain and CNS disorders, Expert Opin. Drug Discov. 4 (2009) 763–784, 10.1517/17460440903018857. [PubMed: 20544003]

[46]. Klawonn AM, Fritz M, Castany S, Pignatelli M, Canal C, Similä F, Tejeda HA, Levinsson J, Jaarola M, Jakobsson J, Hidalgo J, Heilig M, Bonci A, Engblom D, Microglial activation elicits a negative affective state through prostaglandin-mediated modulation of striatal neurons, Immunity 54 (2021) 225–234.e6, 10.1016/j.immuni.2020.12.016. [PubMed: 33476547]

[47]. Bautista DM, Pellegrino M, Tsunozaki M, TRPA1: a gatekeeper for inflammation, Annu. Rev. Physiol. 75 (2013) 181–200, 10.1146/annurev-physiol-030212-183811. [PubMed: 23020579]

[48]. de Montigny C, Cholecystokinin tetrapeptide induces panic-like attacks in healthy volunteers. Preliminary findings, Arch. Gen. Psychiatry 46 (1989) 511–517, 10.1001/archpsyc.1989.01810060031006. [PubMed: 2730276]

[49]. Bradwejn J, Koszycki D, Meterissian G, Cholecystokinin-tetrapeptide induces panic attacks in patients with panic disorder, Can. J. Psychiatr. 35 (1990) 83–85, 10.1177/070674379003500115.

[50]. Bradwejn J, Koszycki D, Comparison of the panicogenic effect of cholecystokinin 30–33 and carbon dioxide in panic disorder, Prog. Neuro-Psychopharmacol. Biol. Psychiatry 15 (1991) 237–239, 10.1016/0278-5846(91)90086-G.

[51]. Zhao L, Xiong Q, Stary CM, Mahgoub OK, Ye Y, Gu L, Xiong X, Zhu S, Bidirectional gut-brain-microbiota axis as a potential link between inflammatory bowel disease and ischemic stroke, J. Neuroinflammation 15 (2018) 339, 10.1186/s12974-018-1382-3. [PubMed: 30537997]

[52]. Ren K, Torres R, Role of interleukin-1beta during pain and inflammation, Brain Res. Rev. 60 (2009) 57–64, 10.1016/j.brainresrev.2008.12.020. [PubMed: 19166877]

[53]. Hui DY, Group 1B phospholipase A2 in metabolic and inflammatory disease modulation, Biochim. Biophys. Acta Mol. Cell Biol. Lipids 2019 (1864) 784–788, 10.1016/j.bbalip.2018.07.001.

[54]. Banchereau J, Pascual V, O'Garra A, From IL-2 to IL-37: the expanding spectrum of anti-inflammatory cytokines, Nat. Immunol. 13 (2012) 925–931, 10.1038/ni.2406. [PubMed: 22990890]

[55]. Cadet JL, Krasnova IN, Walther D, Brannock C, Ladenheim B, McCoy MT, Collector D, Torres OV, Terry N, Jayanthi S, Increased expression of proenkephalin and prodynorphin mRNAs in the nucleus accumbens of compulsive methamphetamine taking rats, Sci. Rep. 6 (2016) 37002, 10.1038/srep37002. [PubMed: 27841313]

[56]. Nakav S, Chaimovitz C, Sufaro Y, Lewis EC, Shaked G, Czeiger D, Zlotnik M, Douvdevani A, Anti-inflammatory preconditioning by agonists of adenosine A1 receptor 3 (2008), e2107, 10.1371/journal.pone.0002107.

[57]. Ohno Y, Kinboshi M, Shimizu S, Inwardly rectifying potassium channel Kir4.1 as a novel modulator of BDNF expression in astrocytes, Int. J. Mol. Sci. 19 (2018) 3313, 10.3390/ijms19113313.

[58]. Iyer SS, Cheng G, Role of interleukin 10 transcriptional regulation in inflammation and autoimmune disease, Crit. Rev. Immunol. 32 (2012) 23–63. [PubMed: 22428854]

[59]. Pasciuto E, Burton OT, Roca CP, Lagou V, Rajan WD, Theys T, Mancuso R, Tito RY, Kouser L, Callaerts-Vegh Z, de la Fuente AG, Prezzemolo T, Mascali LG, Brajic A, Whyte CE, Yshii L, Martinez-Muriana A, Naughton M, Young A, Moudra A, Lemaitre P, Poovathingal S, Raes J, De Strooper B, Fitzgerald DC, Dooley J, Liston A, Microglia require CD4 T cells to complete the fetal-to-adult transition, Cell 182 (2020) 625–640.e24, 10.1016/j.cell.2020.06.026. [PubMed: 32702313]

[60]. Pinho-Ribeiro FA, Borghi SM, Staurengo-Ferrari L, Filgueiras GB, Estanislau C, Verri WA Jr., Bosentan, a mixed endothelin receptor antagonist, induces antidepressant-like activity in mice, Neurosci. Lett. 560 (2014) 57–61, 10.1016/j.neulet.2013.12.018. [PubMed: 24361136]

[61]. Jin J-O, Han X, Yu Q, Interleukin-6 induces the generation of IL-10-producing Tr1 cells and suppresses autoimmune tissue inflammation, J. Autoimmun. 40 (2013) 28–44, 10.1016/j.jaut.2012.07.009. [PubMed: 22921334]

[62]. Hoyer KK, Dooms H, Barron L, Abbas AK, Interleukin-2 in the development and control of inflammatory disease, Immunol. Rev. 226 (2008) 19–28, 10.1111/j.1600-065x.2008.00697.x. [PubMed: 19161413]

[63]. Dienz O, Rincon M, The effects of IL-6 on CD4 T cell responses, Clin. Immunol. 130 (2009) 27–33, 10.1016/j.clim.2008.08.018. [PubMed: 18845487]

[64]. Sofroniew MV, Vinters HV, Astrocytes: biology and pathology, Acta Neuropathol. 119 (2010) 7–35, 10.1007/s00401-009-0619-8. [PubMed: 20012068]

[65]. Chiang CS, Stalder A, Samimi A, Campbell IL, Reactive gliosis as a consequence of interleukin-6 expression in the brain: studies in transgenic mice, Dev. Neurosci. 16 (1994) 212–221, 10.1159/000112109. [PubMed: 7535683]

[66]. Olson JK, Navarro JB, Allen JM, McCulloh CJ, Mashburn-Warren L, Wang Y, Varaljay VA, Bailey MT, Goodman SD, Besner GE, An enhanced Lactobacillus reuteri biofilm formulation that increases protection against experimental necrotizing enterocolitis, Am. J. Physiol. Gastrointest. Liver Physiol. 315 (2018) G408–G419, 10.1152/ajpgi.00078.2018. [PubMed: 29848024]

[67]. Olson JK, Rager TM, Navarro JB, Mashburn-Warren L, Goodman SD, Besner GE, Harvesting the benefits of biofilms: a novel probiotic delivery system for the prevention of necrotizing enterocolitis, J. Pediatr. Surg. 51 (2016) 936–941, 10.1016/j.jpedsurg.2016.02.062. [PubMed: 27032609]

[68]. Fappiano CM, Baraniuk JN, Mil. Med. 185 (2020) e1120–e1127, 10.1093/milmed/usz471. [PubMed: 32009157]

[69]. Picciotto MR, Higley MJ, Mineur YS, Acetylcholine as a neuromodulator: cholinergic signaling shapes nervous system function and behavior, Neuron 76 (2012) 116–129, 10.1016/j.neuron.2012.08.036. [PubMed: 23040810]

[70]. McLin DE 3rd, Miasnikov AA, Weinberger NM, Induction of behavioral associative memory by stimulation of the nucleus basalis, Proc. Natl. Acad. Sci. U. S. A 99 (2002) 4002–4007, 10.1073/pnas.062057099. [PubMed: 11904444]

[71]. Jones BE, Activity, modulation and role of basal forebrain cholinergic neurons innervating the cerebral cortex, Prog. Brain Res. 145 (2004) 157–169, 10.1016/S0079-6123(03)45011-5. [PubMed: 14650914]

[72]. Henderson RF, Barr EB, Blackwell WB, Clark CR, Conn CA, Kalra R, March TH, Sopori ML, Tesfaigzi Y, Ménache MG, Mash DC, Dokladny K, Kozak W, Kozak A, Wachulec M, Rudolph K, Kluger MJ, Singh SP, Razani-Boroujerdi S, Langley RJ, Response of F344 rats to inhalation of subclinical levels of sarin: exploring potential causes of Gulf War illness, Toxicol. Ind. Health 17 (2001) 294–297, 10.1191/0748233701th105oa. [PubMed: 12539875]

[73]. Richtsfeld M, Yasuhara S, Fink H, Blobner M, Martyn JAJ, Prolonged administration of pyridostigmine impairs neuromuscular function with and without down-regulation of acetylcholine receptors, Anesthesiology 119 (2013) 412–421, 10.1097/ALN.0b013e318291c02e. [PubMed: 23563362]

[74]. Forman SA, Miller KW, High acetylcholine concentrations cause rapid inactivation before fast desensitization in nicotinic acetylcholine receptors from torpedo, Biophys. J. 54 (1988) 149–158, 10.1016/S0006-3495(88)82939-4. [PubMed: 3416024]

[75]. Adams SV, Winterer J, Müller W, Muscarinic signaling is required for spike-pairing induction of long-term potentiation at rat schaffer collateral-CA1 synapses, Hippocampus 14 (2004) 413–416, 10.1002/hipo.10197. [PubMed: 15224978]

[76]. Bliss TV, Collingridge GL, A synaptic model of memory: long-term potentiation in the hippocampus, Nature 361 (1993) 31–39, 10.1038/361031a0. [PubMed: 8421494]

[77]. Lev-Lehman E, Evron T, Broide RS, Meshorer E, Ariel I, Seidman S, Soreq H, Synaptogenesis and myopathy under acetylcholinesterase overexpression, J. Mol. Neurosci. 14 (2000) 93–105, 10.1385/JMN:14:1-2:093. [PubMed: 10854041]

[78]. Kaufer D, Friedman A, Seidman S, Soreq H, Anticholinesterases induce multigenic transcriptional feedback response suppressing cholinergic neurotransmission, Chem. Biol. Interact. 119–120 (1999) 349–360, 10.1016/s0009-2797(99)00046-0.

[79]. Dabisch PA, Davis EA, Horsmon MS, Mioduszewski RJ, Development of miotic cross-tolerance between pyridostigmine and sarin vapor, J. Ocul. Pharmacol. Ther. 22 (2006) 323–332, 10.1089/jop.2006.22.323. [PubMed: 17076626]

[80]. Li L, Gunasekar PG, Borowitz JL, Isom GE, Muscarinic receptor-mediated pyridostigmine-induced neuronal apoptosis, Neurotoxicology. 21 (2000) 541–552. https://www.ncbi.nlm.nih.gov/pubmed/11022862. [PubMed: 11022862]

[81]. Kim S, Miller BJ, Stefanek ME, Miller AH, Inflammation-induced activation of the indoleamine 2,3-dioxygenase pathway: relevance to cancer-related fatigue, Cancer 121 (2015) 2129–2136, 10.1002/cncr.29302. [PubMed: 25728366]

[82]. Zhao J, Bi W, Xiao S, Lan X, Cheng X, Zhang J, Lu D, Wei W, Wang Y, Li H, Fu Y, Zhu L, Neuroinflammation induced by lipopolysaccharide causes cognitive impairment in mice, Sci. Rep. 9 (2019), 10.1038/s41598-019-42286-8.

[83]. Yamashita M, Potential role of neuroactive tryptophan metabolites in central fatigue: establishment of the fatigue circuit, Int. J. Tryptophan Res. 13 (2020), 10.1177/1178646920936279.

[84]. Abdel-Rahman A, Abou-Donia S, El-Masry E, Shetty A, Abou-Donia M, Stress and combined exposure to low doses of pyridostigmine bromide, DEET, and permethrin produce neurochemical and neuropathological alterations in cerebral cortex, hippocampus, and cerebellum 67 (2004) 163–192, 10.1080/15287390490264802.

[85]. Madhu LN, Kodali M, Attaluri S, Shuai B, Melissari L, Rao X, Shetty AK, Melatonin improves brain function in a model of chronic Gulf War illness with modulation of oxidative stress, NLRP3 inflammasomes, and BDNF-ERK-CREB pathway in the hippocampus, Redox Biol. 43 (2021), 101973, 10.1016/j.redox.2021.101973. [PubMed: 33933884]

[86]. Sakurai M, Sekiguchi M, Zushida K, Yamada K, Nagamine S, Kabuta T, Wada K, Reduction in memory in passive avoidance learning, exploratory behaviour and synaptic plasticity in mice with a spontaneous deletion in the ubiquitin C-terminal hydrolase L1 gene, Eur. J. Neurosci. 27 (2008) 691–701, 10.1111/j.1460-9568.2008.06047.x. [PubMed: 18279321]

[87]. Lueptow LM, Novel object recognition test for the investigation of learning and memory in mice, J. Vis. Exp. (2017), 10.3791/55718.

[88]. Barker GRI, Warburton EC, When is the hippocampus involved in recognition memory? J. Neurosci. 31 (2011) 10721–10731. https://www.jneurosci.org/content/31/29/10721.short. [PubMed: 21775615]

[89]. Cohen SJ, Munchow AH, Rios LM, Zhang G, Asgeirsdóttir HN, Stackman RW Jr., The rodent hippocampus is essential for nonspatial object memory, Curr. Biol. 23 (2013) 1685–1690, 10.1016/j.cub.2013.07.002. [PubMed: 23954431]

[90]. Chechneva OV, Deng W, Mitochondrial translocator protein (TSPO), astrocytes and neuroinflammation 11 (2016) 1056–1057, 10.4103/1673-5374.187027.

[91]. Chao LL, Rothlind JC, Cardenas VA, Meyerhoff DJ, Weiner MW, Effects of low-level exposure to sarin and cyclosarin during the 1991 Gulf War on brain function and brain structure in US veterans, Neurotoxicology 31 (2010) 493–501, 10.1016/j.neuro.2010.05.006. [PubMed: 20580739]

[92]. Rayhan RU, Stevens BW, Timbol CR, Adewuyi O, Walitt B, VanMeter JW, Baraniuk JN 8 (2013), e58493, 10.1371/journal.pone.0058493.

[93]. Hubbard NA, Hutchison JL, Motes MA, Shokri-Kojori E, Bennett IJ, Brigante RM, Haley RW, Rypma B, Central executive dysfunction and deferred prefrontal processing in veterans with Gulf War illness, Clin. Psychol. Sci. 2 (2014) 319–327, 10.1177/2167702613506580. [PubMed: 25767746]

[94]. Beurel E, Jope RS, Lipopolysaccharide-induced interleukin-6 production is controlled by glycogen synthase kinase-3 and STAT3 in the brain, J. Neuroinflammation 6 (2009) 9, 10.1186/1742-2094-6-9. [PubMed: 19284588]

[95]. Almolda B, Costa M, Montoya M, González B, Castellano B, CD4 microglial expression correlates with spontaneous clinical improvement in the acute Lewis rat EAE model, J. Neuroimmunol. 209 (2009) 65–80, 10.1016/j.jneuroim.2009.01.026. [PubMed: 19246105]

[96]. Christova P, James LM, Carpenter AF, Lewis SM, Johnson RA, Engdahl BE, Georgopoulos AP, Gulf War illness: C-reactive protein is associated with reduction of the volume of hippocampus and decreased fractional anisotropy of the fornix 5 (2020). https://www.jneurology.com/articles/gulf-war-illness-c-reactive-protein-is-associated-with-reduction-of-the-volume-of-hippocampus-and-decreased-fractional-anisotropy-of-the-fornix.pdf.

[97]. Ouali Alami N, Schurr C, Olde Heuvel F, Tang L, Li Q, Tasdogan A, Kimbara A, Nettekoven M, Ottaviani G, Raposo C, Röver S, Rogers-Evans M, Rothenhäusler B, Ullmer C, Fingerle J, Grether U, Knuesel I, Boeckers TM, Ludolph A, Wirth T, Roselli F, Baumann B, NF-κB activation in astrocytes drives a stage-specific beneficial neuroimmunological response in ALS, EMBO J. 37 (2018), 10.15252/embj.201798697.

[98]. Dvoriantchikova G, Barakat D, Brambilla R, Agudelo C, Hernandez E, Bethea JR, Shestopalov VI, Ivanov D, Inactivation of astroglial NF-kappa B promotes survival of retinal neurons following ischemic injury, Eur. J. Neurosci. 30 (2009) 175–185, 10.1111/j.1460-9568.2009.06814.x. [PubMed: 19614983]

[99]. Soung A, Klein R, Astrocytes: initiators of and responders to inflammation, in: Glia in Health and Disease, 2020, p. 109. https://books.google.com/books?hl=en&lr=&id=5kr9DwAAQBAJ&oi=fnd&pg=PA109&dq=Astrocytes+Initiators+of+and+Responders+to+Inflammation&ots=F2kaMJnQrh&sig=9-ACMco212Vb9aFxZ893-fyysiw.

[100]. Krasovska V, Doering LC, Regulation of IL-6 secretion by astrocytes via TLR4 in the fragile X mouse model, Front. Mol. Neurosci. 11 (2018) 272, 10.3389/fnmol.2018.00272. [PubMed: 30123107]

[101]. Engelhart MJ, Geerlings MI, Meijer J, Kiliaan A, Ruitenberg A, van Swieten JC, Stijnen T, Hofman A, Witteman JCM, Breteler MMB, Inflammatory proteins in plasma and the risk of dementia: the Rotterdam study, Arch. Neurol. 61 (2004) 668–672, 10.1001/archneur.61.5.668. [PubMed: 15148142]

[102]. Rainero I, Rubino E, Cappa G, Rota E, Valfrè W, Ferrero P, Fenoglio P, Baci D, D'Amico G, Vaula G, Gallone S, Pinessi L, Pro-inflammatory cytokine genes influence the clinical features of frontotemporal lobar degeneration, Dement. Geriatr. Cogn. Disord. 27 (2009) 543–547, 10.1159/000225962. [PubMed: 19546559]

[103]. Werry EL, Bright FM, Piguet O, Ittner LM, Halliday GM, Hodges JR, Kiernan MC, Loy CT, Kril JJ, Kassiou M, Recent developments in TSPO PET imaging as a biomarker of neuroinflammation in neurodegenerative disorders, Int. J. Mol. Sci. 20 (2019), 10.3390/ijms20133161.

[104]. Cheng C-H, Koo B-B, Calderazzo S, Quinn E, Aenlle K, Steele L, Klimas N, Krengel M, Janulewicz P, Toomey R, Michalovicz LT, Kelly KA, Heeren T, Little D, O'Callaghan JP, Sullivan K, Alterations in high-order diffusion imaging in veterans with Gulf War illness is associated with chemical weapons exposure and mild traumatic brain injury, Brain Behav. Immun. 89 (2020) 281–290, 10.1016/j.bbi.2020.07.006. [PubMed: 32745586]

[105]. Boruch AE, Lindheimer JB, Klein-Adams JC, Stegner AJ, Wylie GR, Ninneman JV, Alexander T, Gretzon NP, Samy B, Van Riper SM, Falvo MJ, Cook DB, Predicting post-exertional malaise in Gulf War illness based on acute exercise responses, Life Sci. 280 (2021), 119701, 10.1016/j.lfs.2021.119701. [PubMed: 34119538]

[106]. Rao RK, Samak G, Protection and restitution of gut barrier by probiotics: nutritional and clinical implications, Curr. Nutr. Food Sci. 9 (2013) 99–107, 10.2174/1573401311309020004. [PubMed: 24353483]

[107]. Valenlia KB, Morshedi M, Saghafi-Asl M, Shahabi P, Abbasi MM, Beneficial impacts of Lactobacillus plantarum and inulin on hypothalamic levels of insulin, leptin, and oxidative markers in diabetic rats, J. Funct. Foods 46 (2018) 529–537, 10.1016/j.jff.2018.04.069.

[108]. Vital M, Karch A, Pieper DH, Colonic butyrate-producing communities in humans: an overview using omics data, mSystems 2 (2017), 10.1128/mSystems.00130-17.

[109]. Soto-Martin EC, Warnke I, Farquharson FM, Christodoulou M, Horgan G, Derrien M, Faurie J-M, Flint HJ, Duncan SH, Louis P, Vitamin biosynthesis by human gut butyrate-producing

bacteria and cross-feeding in synthetic microbial communities, MBio 11 (2020), 10.1128/mBio.00886-20.

[110]. Ma L, Ni Y, Wang Z, Tu W, Ni L, Zhuge F, Zheng A, Hu L, Zhao Y, Zheng L, Fu Z, Spermidine improves gut barrier integrity and gut microbiota function in diet-induced obese mice, Gut Microbes 12 (2020) 1–19, 10.1080/19490976.2020.1832857.

[111]. Geirnaert A, Calatayud M, Grootaert C, Laukens D, Devriese S, Smagghe G, De Vos M, Boon N, Van de Wiele T, Sci. Rep. 7 (2017) 11450, 10.1038/s41598-017-11734-8. [PubMed: 28904372]

[112]. Reyes REN, Zhang Z, Gao L, Asatryan L, Microbiome meets microglia in neuroinflammation and neurological disorders, Neuroimmunol. Neuroinflamm. 2020 (2020), 10.20517/2347-8659.2020.13.

[113]. Cani PD, Bibiloni R, Knauf C, Waget A, Neyrinck AM, Delzenne NM, Burcelin R, Changes in gut microbiota control metabolic endotoxemia-induced inflammation in high-fat diet-induced obesity and diabetes in mice, Diabetes 57 (2008) 1470–1481, 10.2337/db07-1403. [PubMed: 18305141]

[114]. Vargas-Caraveo A, Sayd A, Maus SR, Caso JR, Madrigal JLM, García-Bueno B, Leza JC, Lipopolysaccharide enters the rat brain by a lipoprotein-mediated transport mechanism in physiological conditions, Sci. Rep. 7 (2017) 13113, 10.1038/s41598-017-13302-6. [PubMed: 29030613]

[115]. Kimono D, Bose D, Seth RK, Mondal A, Saha P, Janulewicz P, Sullivan K, Lasley S, Horner R, Klimas N, Chatterjee S, Host Akkermansia muciniphila abundance correlates with Gulf War illness symptom persistence via NLRP3-mediated neuroinflammation and decreased brain-derived neurotrophic factor 15 (2020), 10.1177/2633105520942480.

[116]. Gao J, Xu F, Starlard-Davenport A, Miller DB, O'Callaghan JP, Jones BC, Lu L, Exploring the role of chemokine receptor 6 (Ccr6) in the BXD mouse model of Gulf War illness, Front. Neurosci. 14 (2020) 818, 10.3389/fnins.2020.00818. [PubMed: 32922257]

[117]. Fülling C, Dinan TG, Cryan JF, Gut microbe to brain signaling: what happens in vagus…, Neuron 101 (2019) 998–1002, 10.1016/j.neuron.2019.02.008. [PubMed: 30897366]

[118]. Fröhlich EE, Farzi A, Mayerhofer R, Reichmann F, Jačan A, Wagner B, Zinser E, Bordag N, Magnes C, Fröhlich E, Kashofer K, Gorkiewicz G, Holzer P, Cognitive impairment by antibiotic-induced gut dysbiosis: analysis of gut microbiota-brain communication, Brain Behav. Immun. 56 (2016) 140–155, 10.1016/j.bbi.2016.02.020. [PubMed: 26923630]

[119]. Wang H, Lee I-S, Braun C, Enck P, Effect of probiotics on central nervous system functions in animals and humans: a systematic review, J. Neurogastroenterol. Motil. 22 (2016) 589–605, 10.5056/jnm16018. [PubMed: 27413138]

[120]. Breit S, Kupferberg A, Rogler G, Hasler G, Vagus nerve as modulator of the brain-gut axis in psychiatric and inflammatory disorders 9 (2018) 44.

[121]. Bonaz B, Bazin T, Pellissier S, The vagus nerve at the interface of the microbiota-gut-brain axis, Front. Neurosci. 12 (2018) 49, 10.3389/fnins.2018.00049. [PubMed: 29467611]

[122]. Liu Y, Forsythe P, Vagotomy and insights into the microbiota-gut-brain axis, Neurosci. Res. 168 (2021) 20–27, 10.1016/j.neures.2021.04.001. [PubMed: 33887355]

[123]. Mao J-H, Kim Y-M, Zhou Y-X, Hu D, Zhong C, Chang H, Brislawn CJ, Fansler S, Langley S, Wang Y, Peisl BYL, Celniker SE, Threadgill DW, Wilmes P, Orr G, Metz TO, Jansson JK, Snijders AM, Genetic and metabolic links between the murine microbiome and memory 8 (2020) 53, 10.1186/s40168-020-00817-w.

[124]. Kozlova EV, Carabelli B, Bishay AE, Denys ME, Chinthirla DB, Tran JD, Hsiao A, Nieden NZ, Curras-Collazo MC, Persistent exercise fatigue and associative learning deficits in combination with transient glucose dyshomeostasis in a GWI mouse model, Life Sci. (2021) 120094, 10.1016/j.lfs.2021.120094. [PubMed: 34710444]

Fig. 1.

GW exposure model and endpoints. Four experimental groups of adult mice were used: a sham-treated control (CON), a sham-treated control that also received restraint stress (CON/S), and two GW groups that received one of two doses of PB P.O.: 6.5 mg/kg b.i.d. (GW1) and 8.7 mg/kg (GW2), plus topical DEET and PER as well as restraint stress. The exposure regime was given 5 d/week followed by 2 d rest for 4 wk. Animals were first tested on metabolic, behavior and exercise endpoints as described in an accompanying paper [124]. At sacrifice, 6.6 months later, tissues were collected and used for IL-6 ELISA, GFAP immunohistochemistry, PCR analysis of brain gene expression of neuroinflammatory and neuropathic pain related pathways, serum endotoxin and fecal 16S rRNA next generation sequencing (NGS). Fecal pellets were collected before intervention (PRE) and at PT 3 and 188. DEET, N,N-diethyl-meta-toluamide; GFAP, glial fibrillary acidic protein; PB, pyridostigmine bromide; PER, permethrin; PT, post-treatment; T, time-point; TRT, treatment. GW1, 6.5 mg/kg b.i.d.; GW2, 8.7 mg/kg.

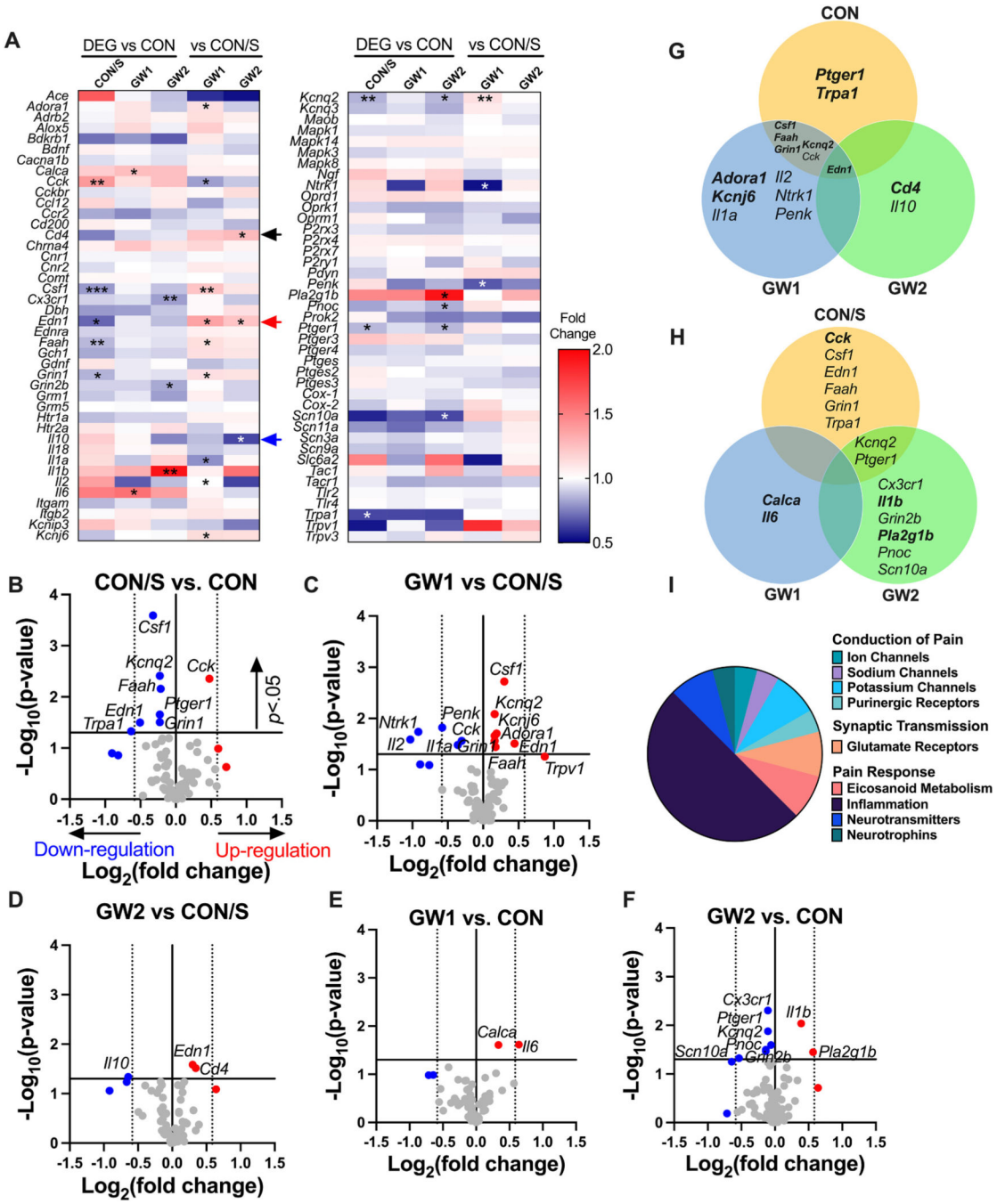

Fig. 2.

Two neuroinflammatory transcriptional phenotypes induced by GW agent exposure. (A) cDNA samples obtained from pooled unilateral brain (PFC, hippocampus, hypothalamus) at PT 199 were analyzed using PCR array. Heat map shows representation of differentially expressed genes (DEGs) normalized to reference genes and fold-change relative to CON or CON/S (double gradient, blue indicates downregulated; red indicates upregulated). Genes were deemed significantly deregulated if they met the criterion of cutoff $p < .05$ vs control group. GW1 and GW2 groups showed different profiles of DEGs relative to CON/S and

each other. *statistical significance relative to CON/S or CON; *$p < .05$, **$p < .01$, ***$p < .001$. Red arrow, upregulated *Edn1* in GW1 and GW2; black arrow, upregulated *Cd4* in GW2; blue arrow, downregulated *Il10* in GW2. (B–F) Volcano plots of DEGs demonstrating up- or down-regulated genes. Vertical lines indicate using ±1.5-fold thresholds compared to corresponding control group indicated; up-regulated genes (red dots to the right of 0), or down-regulated genes (blue dots to the left of 0). The horizontal line indicates threshold for significant change at $p < .05$. (G–H) Venn diagrams indicating DEGs relative to CON/S (G) and CON (H). Bolded genes are up-regulated relative to the groups indicated (I). Pie chart showing the proportion of genes altered in each of 3 pathways. Values are expressed as mean ± s.e.m. *significantly different from CON/S, $p < .05$. (A–I) $n = 3–6$ mice/group. DEG, differentially expressed genes. GW1, 6.5 mg/kg b.i.d.; GW2, 8.7 mg/kg. (For interpretation of the references to color in this figure legend, the reader is referred to the web version of this article.)

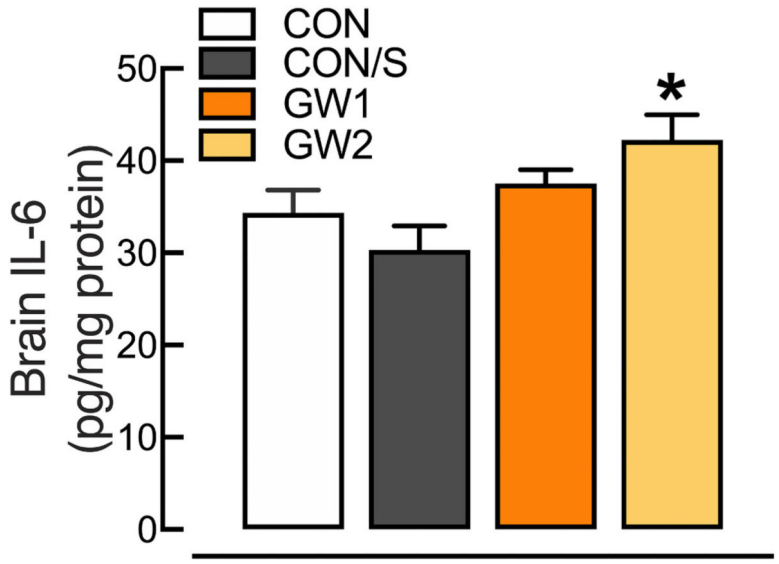

Fig. 3.

Brain levels of IL-6 protein are significantly elevated in GW2 relative to CON/S. Homogenized whole-brain samples obtained at PT 199 were analyzed for IL-6 using ELISA. Values are expressed as mean ± s.e.m. *significantly different from CON/S, $p < .05$. n = 3/group. GW1, 6.5 mg/kg b.i.d.; GW2, 8.7 mg/kg.

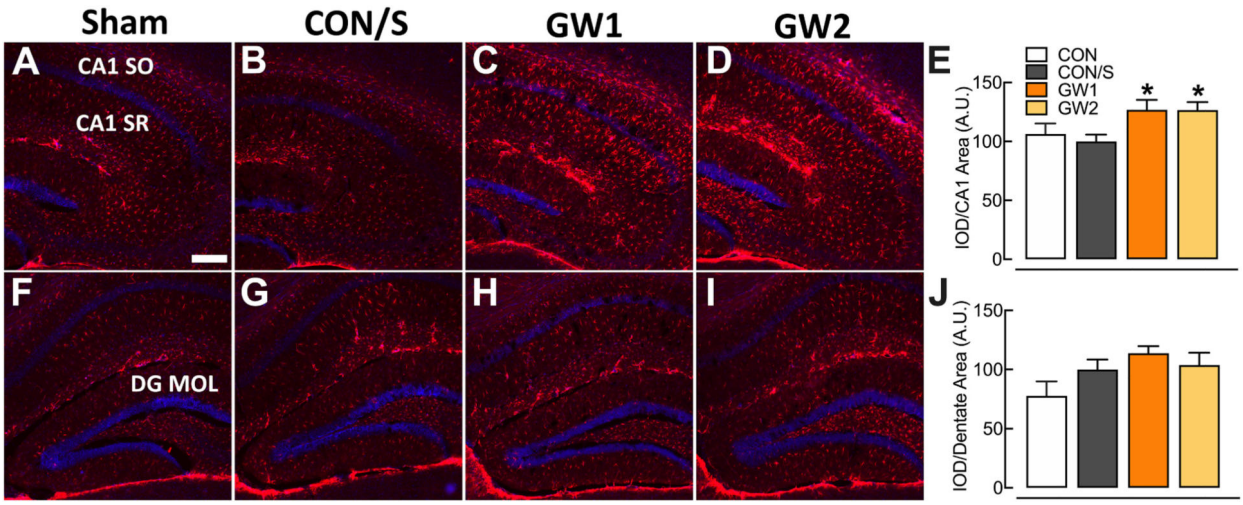

Fig. 4.

GW1 and GW2 agents induce hypertrophy in GFAP-positive astrocytes in the hippocampus. Micrographs demonstrating GFAP-positive astrocytes from the CA1 (A–D) and DG (F–I) subfields. The bar graphs compare the mean integrated optical density (IOD) of GFAP immunoreactivity normalized to the total area analyzed in the CA1 SR + SO (E) and dentate gyrus inner and outer molecular layers (MOL) (J) relative to CON/S. Values are expressed as mean ± s.e.m. *significantly different from CON/S; *$p < .05$. $n = 8–11$/group. A.U., arbitrary units; DG, dentate gyrus; MOL, molecular layer; SO, stratum oriens; SR, stratum radiatum. GW1, 6.5 mg/kg b.i.d.; GW2, 8.7 mg/kg. Scale bar = 2000 μm.

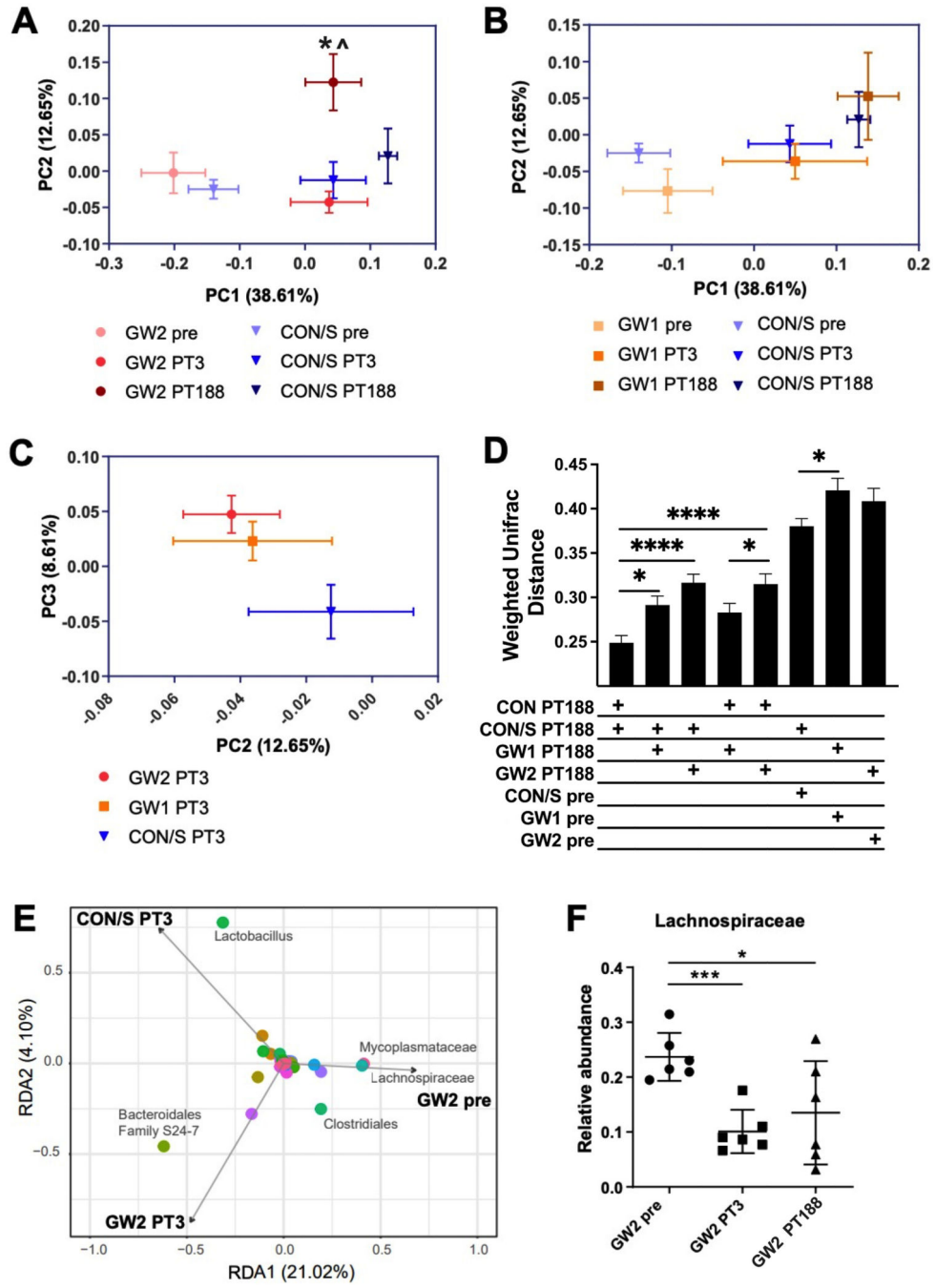

Fig. 5.

Different Gut Microbiome Community Structure in GW1 and GW2. (A–C) Principal coordinates analysis (PCoA) of weighted Unifrac distance between fecal communities of indicated groups of mice. Percent variance explained is in parentheses by PC axis. *significant difference between GW2 pre and PT 188, $p < .05$ and ^significant difference between GW2 PT3 and PT188, $p < .05$. (D) All pairwise weighted Unifrac distances between indicated groups (+) at PT 188 shows significant effects of GW agents on microbiome community structure. (E) Redundancy analysis (RDA) of microbial

composition before (pre) and after treatment (PT3) at genus level. The 50 most abundant genera were selected for this analysis. Colors were randomly assigned to individual taxa. RDA indicates higher abundance of Bacteroidales with GW2 and of Lactobacillus with CON/S. (F) Relative abundance of Lachnospiraceae in fecal microbiomes is downregulated in GW2 PT3 and PT188 vs GW2 pre. *$p < .05$, ***$p < .001$. Values are expressed as mean ± s.e.m. $n = 5–10$/group. GW1, 6.5 mg/kg b.i.d.; GW2, 8.7 mg/kg; PT, post-treatment day; pre, pre-treatment.

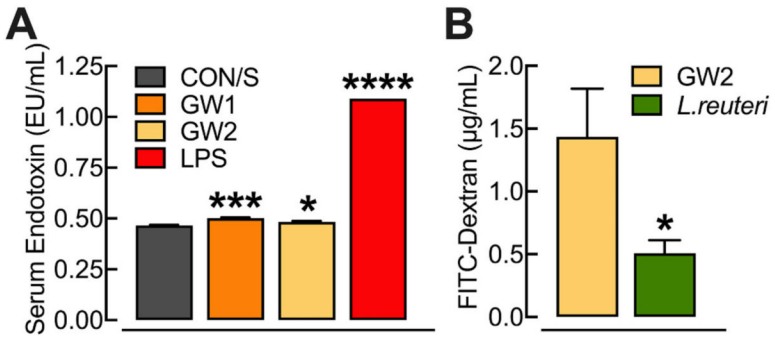

Fig. 6.

GW agent exposure produces mild endotoxemia and *Lactobacillus reuteri* supplementation improves gut barrier function. (A) Systemic endotoxin levels measured in serum collected at sacrifice at PT 199 show significantly increased endotoxemia in GW1 and GW2 that is mild compared to LPS-treated mice. (B) Intestinal permeability was measured using a FITC-dextran assay in germ-free mice receiving transplantation of fecal microbiota collected from GW2 before sacrifice or in germ-free mice inoculated with *L. reuteri* cultures. Values are expressed as mean ± s.e.m. *compared to CON/S (A) or GW2 (B), *$p < .05$, ***$p < .001$, ****$p < .0001$. $n = 1–4$/group; EU, endotoxin units; FITC, fluorescein isothiocyanate; GW1, 6.5 mg/kg b.i.d.; GW2, 8.7 mg/kg; LPS, lipopolysaccharide.

Table 1

Summary of symptoms in GW1 and GW2 phenotypes and biomarkers relative to CON/S.

	GW1	GW2
Neurological		
Anxiety - elevated plus maze	−	−
Anxiety - Suok	−	−
Anxiety - open field test	−	−
Cognitive - novel object recognition	+	−
Cognitive - passive avoidance	+	+
Cognitive - Barnes maze	−	+
Mood - anhedonia/self-care - sucrose splash test		
Mood - depression/behavioral despair - forced swim test	+	−
Mood - depression/behavioral despair - tail suspension test	−	−
Pain - hot plate test	−	−
Fatigue/sleep - exercise fatigue	−	+
Other		
Metabolic - insulin insensitivity - insulin tolerance test	−	+
Metabolic - post-exercise lactatemia	−	−
Metabolic - post-exercise glycemia	−	−
Metabolic - elevated body weight	−	−
Metabolic - reduced lean/fat mass	−	−
Sensorimotor - rotarod	−	−
Sensorimotor - Suok	−	−
Locomotion - open field test	−	−
Biomarkers		
Gut dysbiosis	+	+
Endotoxemia - limulus amebocyte lysate assay	+	+
Neuroinflammation - hypertrophied GFAP-positive astrocytes	+	+
Neuroinflammation - Interleukin-6	−	+
Neuroinflammation/neuropathic pain transcripts	+	+

Categories are based on symptom groups in Kansas case definitions [23]. Scores indicate normal parameters (−) or alterations (+) relative to CON/S.